Silicon Carbide Benefits and Advantages for Power Electronics Circuits and Systems

AHMED ELASSER, MEMBER, IEEE, AND T. PAUL CHOW, SENIOR MEMBER, IEEE

Invited Paper

Silicon-based power semiconductor devices, ranging from diodes, thyristors, gate turn-off thyristors, metal–oxide–semiconductor field-effect transistors, and, more recently, insulated-gate bipolar transistors, integrated gate-commutated thyristors, and metal–oxide–semiconductor turn-off thyristors, are the workhorse of power electronic systems and circuits. Silicon offers multiple advantages to power circuit designers, but at the same time suffers from limitations that are inherent to silicon material properties, such as low bandgap energy, low thermal conductivity, and switching frequency limitations. Wide bandgap semiconductors, such as silicon carbide (SiC) and gallium nitride (GaN), provide larger bandgaps, higher breakdown electric field, and higher thermal conductivity. Power semiconductor devices made with SiC and GaN are capable of higher blocking voltages, higher switching frequencies, and higher junction temperatures than silicon devices. SiC is by far the most advanced material and, hence, is the subject of attention from power electronics and systems designers. This paper looks at the benefits of using SiC in power electronics applications, reviews the current state of the art, and shows how SiC can be a strong and viable candidate for future power electronics and systems applications.

Keywords*—*Applications, converters, devices, material, power devices, power electronics, power systems, silicon carbide.

I. General Background and Introduction

Silicon-based power devices have long dominated the power electronics and power systems applications. There is a host of bipolar, unipolar, controlled, uncontrolled, and metal–oxide–semiconductor (MOS)-gated Si devices that are widely used by power electronics and power systems designers. Examples of such devices are diodes (p–i-n and Schottky rectifiers), thyristors, gate turn-off thyristors (GTOs), gate-controlled thyristors (GCT), bipolar junction transistors (BJTs), insulated-gate bipolar transistors (IGBTs), and power metal–oxide–semiconductor field-effect transistors (MOSFETs). Large-area devices that are capable of handling thousands of amperes and kilovolts are now available from a large number of manufacturers. MOS-gated devices such as IGBTs are now able to handle voltages up to 6 kV and currents up to 1200 A [1]. IGBTs are being widely used for motor drives, resonant converters, and power supplies. IGBTs offer low switching losses, high switching frequency operation, and a simplified gate circuit [2]–[4]. GTOs and thyristors, on the other hand, are still widely used for very high power applications, such as power systems conditioning equipment, dynamic voltage regulators, transfer switches, and large direct-current (dc) rectifiers [5]–[8]. Power MOSFETs found great usage within the power-supply community. Their ease of drive and their low switching losses makes them perfect for very high switching frequency applications [9]. They are also used in resonant converters switching up to 1 MHz and in some cases in low power inverter applications [10]. Moreover, they are widely used as synchronous rectifiers in low output voltage power supplies [11]. MOSFETs have been hindered for a long time by their relatively high conduction losses due to their high on-state resistance, R_{dson}. As the blocking voltage (BV) increases, so does their on-state resistance R_{dson}, hence, making MOSFETs less attractive for high-voltage applications (beyond 600 V). Recent enhancements in power MOSFET technology such as the CoolMOS [12] allow for substantial reduction of the conduction losses.

The need for faster devices with high voltage and high switching frequency capability is growing, especially for advanced power conversion. Applications where devices are required to operate at higher than 150 °C junction temperature, high voltages, high switching frequencies, and high power densities are growing especially for military applications. Silicon-based devices are not able to meet

Manuscript received September 14, 2001; revised December 26, 2001. This work was supported by the Defense Advanced Research Projects Agency under Contract MDA972-98-C-0001, the Office of Naval Research under Grant N00014-95-1-1302, and the National Science Foundation under Award EEC-9731677.

A. Elasser is with General Electric Corporate Research and Development, Niskayuna, NY 12309 USA (e-mail: elasser@crd.ge.com).

T. Paul Chow is with the Department of Electrical, Computer, and Systems Engineering, Rensselaer Polytechnic Institute, Troy, NY 12180 USA (e-mail: chowt@rpi.edu).

Publisher Item Identifier S 0018-9219(02)05576-7.

Table 1
Physical Properties of Important Semiconductors for High-Voltage Power Devices

Material	E_g (eV)	n_i (cm^{-3})	ε_r	μ_n ($cm^2/V \cdot s$)	E_c (MV/cm)	v_{sat} (10^7 cm/s)	λ (W/cm·K)	*Direct/ Indirect*
Si	1.1	1.5×10^{10}	11.8	1350	0.3	1.0	1.5	I
Ge	0.66	2.4×10^{13}	16.0	3900	0.1	0.5	0.6	I
GaAs	1.4	1.8×10^{6}	12.8	8500	0.4	2.0	0.5	D
GaP	2.3	7.7×10^{-1}	11.1	350	1.3	1.4	0.8	I
InN	1.86	$\sim 10^3$	9.6	3000	1.0	2.5	-	D
GaN	3.39	1.9×10^{-10}	9.0	900	3.3	2.5	1.3	D
3C-SiC	**2.2**	**6.9**	**9.6**	**900**	**1.2**	**2.0**	**4.5**	**I**
4H-SiC	**3.26**	**8.2×10^{-9}**	**10**	**720[a] 650[c]**	**2.0**	**2.0**	**4.5**	**I**
6H-SiC	**3.0**	**2.3×10^{-6}**	**9.7**	**370[a] 50[c]**	**2.4**	**2.0**	**4.5**	**I**
Diamond	5.45	1.6×10^{-27}	5.5	1900	5.6	2.7	20	I
BN	6.0	1.5×10^{-31}	7.1	5	10	1.0*	13	I
AlN	6.1	$\sim 10^{-31}$	8.7	1100	11.7	1.8	2.5	D

Note: *a* — mobility along a-axis, *c* — mobility along c axis, *— estimate.

these stringent requirements without costly cooling systems, large number of devices in series and parallel, and costly active or passive snubbers. The latter adds to the overall size and weight, a mostly undesirable feature of silicon-based power converters. Wide-bandgap-based semiconductor devices such as silicon carbide and gallium nitride offer multiple advantages for power electronic designers [13], [14]. The superior physical properties of these semiconductors offer a lower intrinsic carrier concentration (10–35 orders of magnitude), a higher electric breakdown field (4–20 times), a higher thermal conductivity (3–13 times), a larger saturated electron drift velocity (2–2.5 times), when compared to silicon (see Table 1). Silicon carbide in particular has been the focus of a number of research groups and organizations in the past 15 years [15]. Its wide bandgap energy of 2.2–3.3 eV is larger than the 1.1-eV bandgap of silicon. In addition, SiC has a higher electric breakdown field of 3×10^6 V/cm, which is an order of magnitude larger than that of silicon. The higher breakdown field allows a ten times reduction in drift layer thickness; hence, lessening the minority carrier charge storage and greatly increasing the switching frequency of bipolar devices. Its high carrier saturation velocity of 2×10^7 cm/s is also an order of magnitude larger than silicon's. Its high thermal conductivity of 4.9 W/cm·K enhances heat dissipation and coupled with the wide bandgap energy allows for power efficient high temperature operation up to 350 °C [16]. According to various figures of merit, SiC comes out on top of silicon and gallium arsenide as the material of choice for power devices [17].

Despite all these advantages, silicon carbide has not been adopted for power devices until recently. Difficulty with material processing, presence of crystal defects such as micropipes and dislocations, and lack of abundant wafer suppliers have all contributed to a lack of rapid progress in making SiC power devices commercially available and widely used by the power electronics community [13]. In the past 15 years, SiC research and development has accelerated in the United States and around the world. Commercial wafers (up to 75 mm) are now available in the United States from a number of manufacturers [18]. Several industrial research groups and universities have been working diligently on the development of SiC power devices and on overcoming the inherent difficulties associated with material quality, properties, fabrication, process, and packaging. Devices such as Schottky and p–i-n diodes are well advanced and some manufacturers are now offering SiC Schottky diodes rated as high as 600 V and 10 A [19]. Controllable devices such as GTOs and BJTs have also been extensively studied and many research groups have reported results on GTOs with voltage ratings as high as 3 kV and current ratings as high as 10 A [20], [21]. Although these initial devices are small compared to their Si counterpart, they are shown to offer superior characteristics, and it is only a matter of time before large area devices will be available [22]. Other popular devices such as MOSFETs and IGBTs are still facing some challenges, particularly in the area of oxide growth and carrier mobility. The low effective MOS channel mobility in SiC makes it difficult to build low threshold and high current carrying power MOSFETs [23].

II. SiC Power Devices—State of the Art in Material and Devices

A. Silicon Carbide Characteristics

SiC has over 150 polytypes, but only the 6H– and 4H–SiC polytypes are available commercially in both bulk wafers and custom epitaxial layers. Between the two polytypes, 4H–SiC is preferred for power devices primarily because of its high carrier mobility, particularly in c-axis direction and its low dopant ionization energy. In addition, the high electric breakdown field of SiC allows for thinner epitaxial layers to support the high BV in power devices. A 5000-V power device would require only 40–50 μm drift layer, as opposed to almost 500 μm in the case of silicon. This smaller drift layer leads to low drift resistance; hence, low forward drop and conduction losses. SiC thermal conductivity of about 5 W/cm·K allows for high junction temperature operation

Table 2
Normalized Unipolar Figures of Merit of Important Semiconductors for High-Voltage Power Devices

Material	λ	JM $(E_c v_{sat}/\pi)^2$	MJM λ*JM	KM $\lambda(v_{sat}/\varepsilon_r)^{1/2}$	Q_{F1} $\lambda\sigma_A$	Q_{F2} $\lambda\sigma_A E_c$	BM (Q_{F3}) $\varepsilon_r \mu E_c^3$	BHFM μE_c^2
Si	1	1	1	1	1	1	1	1
Ge	0.4	0.03	0.012	0.20	0.06	0.02	0.2	0.3
GaAs	0.33	7.1	2.4	0.45	5.2	6.9	15.6	10.8
GaP	0.53	37	20	0.7	10	40	16	5
InN	-	58	-	-	-	-	46	19
GaN	0.87	760	655	1.6	560	6220	650	77.8
3C-SiC	3	65	195	1.6	100	400	33.4	10.3
4H-SiC	3	180	540	4.61	390	2580	130	22.9
6H-SiC	3	260	780	4.68	330	2670	110	16.9
Diamond	13.3	2540	33800	32.1	54860	1024000	4110	470
BN	8.7	1100	9700	11	715	23800	83	4
AlN	1.7	5120	8700	21	52890	2059000	31700	1100

Table 3
Bipolar Figure of Merit Applied to the Power p-i-nJunction Rectifier (Calculated at $J_F = 100$ A/cm^2, $BV = 1000$ V)

Name	N_d (cm^{-3})	W_{N^-} (μm)	V_F (V)	J_{ond} (A/cm^2)	J_{off} (A/cm^2)	t_s (μs)	t_{f1} (μs)	t_{f2} (μs)	E_{off} (mJ)	f_{min} (KHz)
Si	1.3×10^{14}	100	0.88	9.7	2×10^{-5}	7×10^{-3}	0.81	0	5.4×10^{-3}	-
Ge	4.4×10^{13}	285	0.60	8.3	8×10^{-2}	7.6×10^{-3}	1.8	0	6.2×10^{-3}	0
3C-SiC	3.8×10^{15}	33.1	2.00	42.8	2×10^{-15}	4.4×10^{-3}	0.2	2.2×10^{-3}	2×10^{-2}	1.62
6H-SiC	1.6×10^{16}	23.9	2.65	46.2	3×10^{-21}	1.0×10^{-2}	0.14	4.6×10^{-3}	5.5×10^{-3}	1.82
Diamond	1.2×10^{17}	72.0	5.21	93.4	5×10^{-44}	2.6×10^{-5}	0.02	1×10^{-2}	1.1×10^{-3}	4.12

Table 4
Bipolar Figure of Merit Applied GTO Thyristor (Calculated at $J_F = 100$ A/cm^2, $BV = 1000$ V, Turn-Off Gain of 4)

Name	N_d (cm^{-3})	W_{N^-} (μm)	V_F (V)	J_{off} (A/cm^2)	β_{max}	J_{ATO} (A/cm^2)	t_s (μs)	t_{f1} (μs)	E_{off1} (mJ)	E_{on1} (mJ)	f_{min} (KHz)
Si	1.3×10^{14}	144	0.99	2.9×10^{-5}	5.8	1.1×10^{3}	0.3	0.58	9.6	24	-
Ge	4.4×10^{13}	285	0.60	1.1×10^{-1}	5.5	3.0×10^{3}	0.26	0.62	10	24	<53.7
3C-SiC	3.8×10^{15}	33.1	2.00	3.9×10^{-13}	25.1	2.6×10^{3}	1.4×10^{-2}	0.29	4.8	24	10.5
6H-SiC	1.6×10^{16}	23.9	2.65	7.9×10^{-19}	88	1.8×10^{4}	1.1×10^{-2}	0.19	3.1	24	12.6
Diamond	1.2×10^{17}	72.0	5.21	1.7×10^{-41}	2.3×10^{4}	8.0×10^{8}	4.1×10^{-5}	0.029	0.48	24	23.2

and for efficient thermal management. Another important parameter is carrier lifetime. SiC, like silicon, is an indirect bandgap semiconductor, whereas GaN, like GaAs, are direct bandgap semiconductors. Consequently, SiC has minority carrier lifetimes much longer than those in GaN. Experimentally, recombination lifetimes >1 μs have been extracted in 4H–SiC [24].

B. SiC Figures of Merit

To quantify the performance enhancement possible with SiC, several unipolar and bipolar figures of merit have been proposed [17], [25]–[28]. In Tables 2 and 3, various unipolar and bipolar figures of merit for the semiconductors are shown and SiC offers more than an order of magnitude improvement over silicon. Bipolar transistors can be classified into two groups: those with an odd number of junctions and those with an even number of junctions. The BJT has an even number of junctions and hence its on-state voltage can be minimized through cancellation of junction voltages when it is in saturation. In this case, SiC clearly excels over Si over all switching frequencies and the power dissipation is clearly smaller in SiC transistors, as shown in Table 3. By contrast, the IGBT [29], which is the dominant silicon power transistor structure, has an odd number of junctions in its structure and its forward drop cannot be reduced to less than a diode drop. Since SiC has a large diode turn-on voltage due to its larger bandgap, its conduction loss cannot be less than the silicon device at low to medium current density and only yields a lower total power loss when the switching frequency exceeds a certain frequency $f_{\min}$ [26], [27]. This $f_{\min}$, at which the conduction loss is equal to the switching loss (at 50% duty cycle), has been considered as the bipolar figure of merit and, in the case of a 1000-V IGBT, is about 20 kHz for SiC when compared to silicon, as illustrated in Table 4.

C. SiC Power Devices

One of the basic building blocks of a power circuit is the half-bridge circuit (see Fig. 1) in which two modules are connected in series and each module is composed of a three-terminal switch and two-terminal flyback rectifier connected in

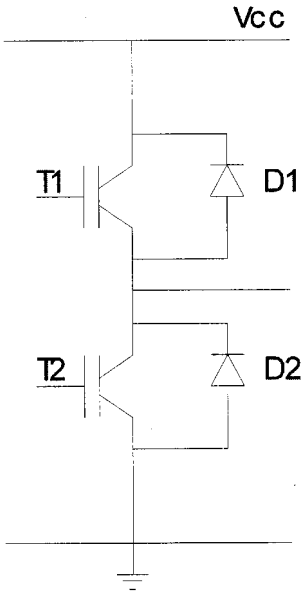

Fig. 1. Half-bridge inverter leg.

antiparallel. Thus, it can be seen that both two- and three-terminal switching devices are needed. There are basically two families of two- and three-terminal power semiconductor switching devices—the Schottky rectifier and the power FET representing the unipolar family and the junction rectifier, the BJT and the thyristor belonging to the bipolar family. Also, for three-terminal devices, depending on whether current or voltage signal is used for control, they can further be classified into two more branches. While traditional power device switches use current for control (such as power BJT, silicon-controlled rectifier (SCR), and GTO [30]), modern power devices (such as the power MOSFET, IGBT, and MOS-controlled thyristor [29]) prefer the usage of a MOS voltage control for reduced control circuit complexities and enhanced device diagnostics features, but at the expense of device yield limitations from gate oxide failures.

1) Power Rectifiers: Generally, high-voltage power rectifiers are categorized into two classes—the unipolar Schottky rectifier and the bipolar junction rectifier [29]. The schematic cross sections of the basic structures of these two rectifiers are shown in Fig. 2(a) and (b). High-voltage Schottky rectifiers offer fast switching speed, but suffer from high on-state voltage drop and on-resistance because mostly majority carriers participate in its forward conduction. By contrast, the p–i-n junction rectifier has low forward drop and high current capability due to conductivity modulation, but has slow reverse recovery characteristics due to minority carrier storage. To combine the best features of these two rectifiers, hybrid rectifier structures, such as the junction barrier Schottky, merged p–i-n/Schottky, and MOS barrier Schottky rectifiers have also been proposed. Whether a unipolar or a bipolar rectifier is preferred depends on many application parameters, such as reverse BV, forward current density, maximum allowable reverse current density, operating temperature, and switching frequency. The particular device type is often chosen to either minimize the total

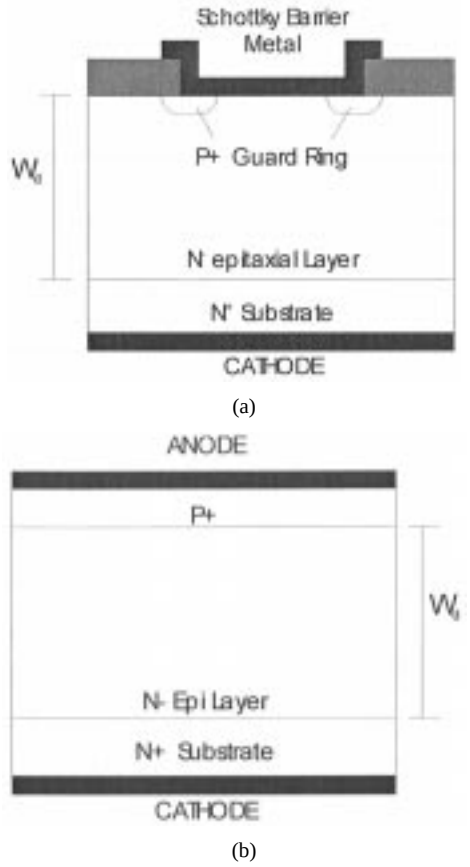

Fig. 2. (a) Schottky rectifier cross section. (b) p–i-n junction rectifier cross section.

power dissipation or maximize the safe operating area (SOA) during device turn-on or turn-off. If we only focus on forward conduction, we note that the turn-on voltage of silicon rectifier is only 0.7 V while that of the 4H–SiC rectifier is about 2.5 V (the turn-on voltage is approximately 75% of the bandgap).

a) Schottky rectifiers: The Schottky barrier rectifiers are attractive due to their fast switching speed. This device exhibits fast reverse recovery with no reverse current and no forward overvoltage transient because the forward current transport is mainly by majority carriers. We have included recent published experimental results [31]–[39] in Fig. 3. As seen in this figure, experimental SiC Schottky rectifiers have achieved significant improvement over Si counterparts, but they are still far from the theoretical predictions. The highest reverse BV reported so far for a 4H–SiC Schottky rectifier is about 3000 V. The power dissipation (P_D) of a Schottky rectifier consists of only the on-state conduction loss and the off-state leakage loss and it can be optimized with the choice of Schottky barrier height

$$P_D = J_F * V_F * D + J_R * V_R * (1 - D) \qquad (1)$$

where D is the duty cycle, J_F is the forward conduction current density, J_R is the reverse current density, V_F is the total voltage drop, and V_R is the reverse BV. Fig. 4 shows the calculated power dissipation of 1000-V Schottky rectifiers on 6H–SiC and 4H–SiC with three different barrier heights and

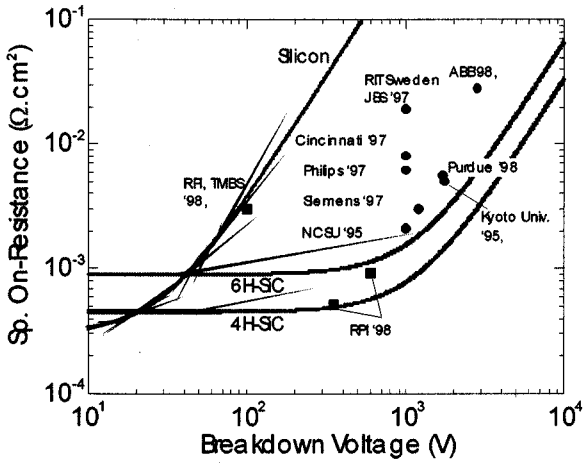

Fig. 3. Specific on-resistance versus reverse BV for Si, 6H–, and 4H–SiC Schottky.

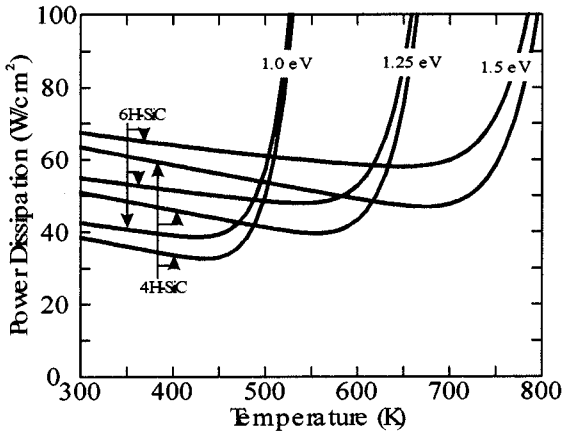

Fig. 4. Estimated power dissipation for 1000-V 4H– and 6H–SiC Scottky diodes.

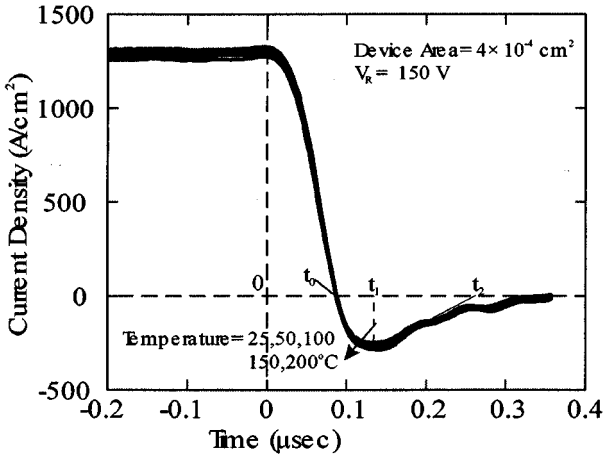

Fig. 5. Reverse recovery current versus temperature for an 1100-V 4H–SiC p–i-n diode.

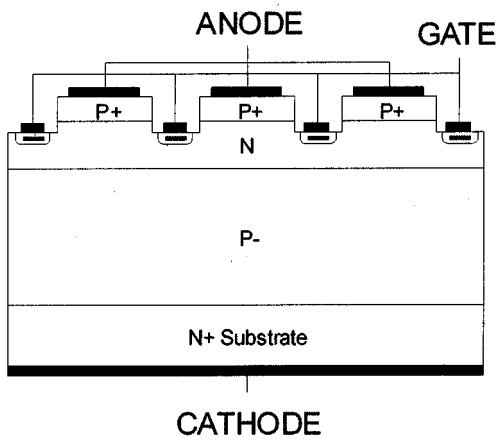

Fig. 6. Cross section of a SiC thyristor.

with $J_F = 100$ A/cm^2, $V_R = 500$ V, and $D = 0.5$ (or 50%). For a silicon Schottky with the same voltage rating, the power dissipation has been estimated to be at least an order of magnitude higher. The estimated power dissipation is based on the results for a 20-V Si Schottky diode under similar conditions as presented in [29, p. 144]. The main reason for the higher power dissipation for Si devices is the higher conduction losses (due to higher V_F) at low temperatures. At higher temperatures (>100 °C), the off-state standby power increases substantially (due to higher V_R).

b) p-i-n junction rectifiers: The p–i-n junction rectifier is the dominant silicon power rectifier structure. The forward voltage drop of a p–i-n junction rectifier consists of the drop across the middle region (V_m) and the drops across the two end junctions according to

$$V_F = V_{P+} + V_m + V_{N+} \tag{2}$$

where V_{P+} and V_{N+} are the voltage drops across the anode and cathode junctions, respectively, and the mid-region drop V_m depends strongly on carrier recombination lifetimes and can be expressed as transcendental functions of d/L_a (see [30, Eq. (3.81)]). The switching of the junction rectifier can be modeled with a charge-control model and unlike the low-voltage diodes, the switching from the forward to reverse conditions usually goes through a constant di/dt ramp [29]. Besides the circuit-imposed di/dt, the reverse recovery time is also dependent on lifetime. Due to the reduced drift region width with SiC, a less demanding lifetime is needed to achieve conductivity modulation. Recent experimental data have been included in Fig. 5 to assess the degree of optimization of these devices. The reverse recovery current waveforms of both epitaxial and implanted junction rectifiers have an interesting temperature dependence that has not been seen in Si devices [42]. In Fig. 5, typical reverse recovery current waveforms of a 1100-V p$^+$n implanted SiC diode are measured up to 200 °C. Interestingly, the reverse recovery charge (Q_{rr}) and recovery time (t_{rr}) remains constant with increasing temperature, which may indicate the deepness of the energy level of the recombination centers. Also, their values (18 nC and 0.1 μs, respectively) are significantly lower than those for an equivalent silicon rectifier of the same voltage rating.

2) Power Thyristors:

a) SCRs: For SiC, due to the difficulties in heavy p-type doping in the substrate, an n+ substrate is usually

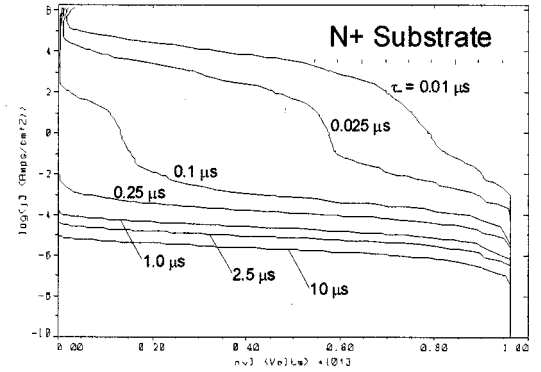

(a)

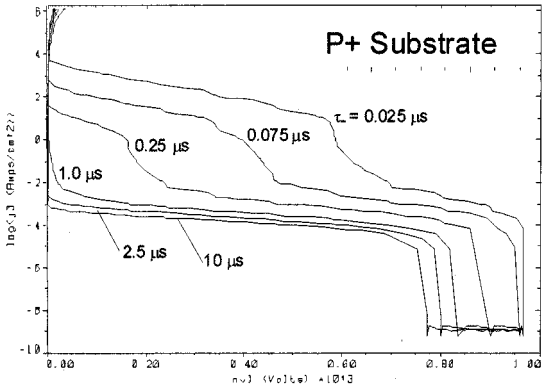

(b)

Fig. 7. (a) Simulated holding current for a 5000–V 4H–SiC n–p–n–p SCR. (b) Simulated holding current for a 5000-+V 4H–SiC p–n–p–n SCR.

used. Consequently, the actual thyristor structure studied is complementary to that of conventional silicon SCRs. Fig. 6 shows the schematic cross section of a SiC thyristor. From device considerations, the lower transistor being n–p–n improves the BV_{CEO} and SOA, but the upper p–n–p transistor requires a larger gate current to turn on due to lower n-base sheet resistance and current gain. To quantify the performance between p–n–p–n and n–p–n–p SCRs, we have calculated their respective holding currents, as illustrated in Fig. 7(a) and (b) for 5000-V 4H–SiC devices. Clearly, the SCR with the cathode as substrate is favored. Once triggered on, the thyristor on-state characteristics strongly resemble that of a p–i-n junction rectifier [29], [30]. With both the upper and lower base conductivities modulated with carriers injected from the anode and cathode, the forward drop approaches that of the p–i-n diode.

b) GTOs: To facilitate turn-off, the thyristor can be designed so that a gate current (in opposite direction to the gate triggering current) is used without device commutation (or anode-cathode voltage reversal). Symmetric and asymmetric 6H- and 4H–SiC GTOs reported in the literature have BVs up to 3000 V and 6 A at present [20]–[22]. It has been demonstrated early that SiC thyristors can operate at much higher temperatures than their silicon counterpart [20]. In Fig. 8, the current–voltage (I–V) characteristics of 4H–SiC GTOs up to 300 °C are shown [20]. Most of the published thyristor structures use epi p+ emitter and n+ substrates. The effect of the

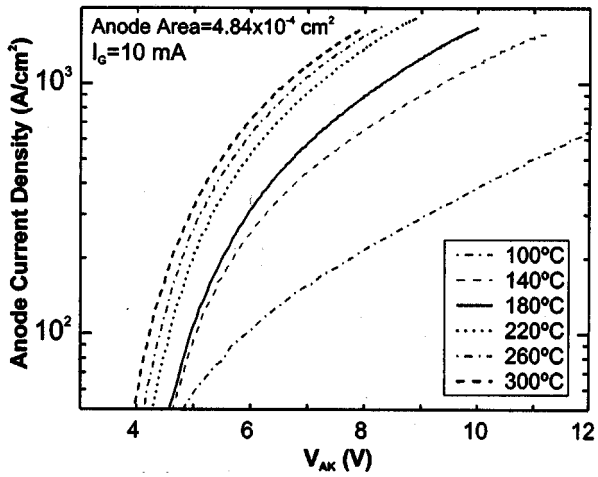

Fig. 8. Forward I–V characteristics of a 4H–SiC GTO.

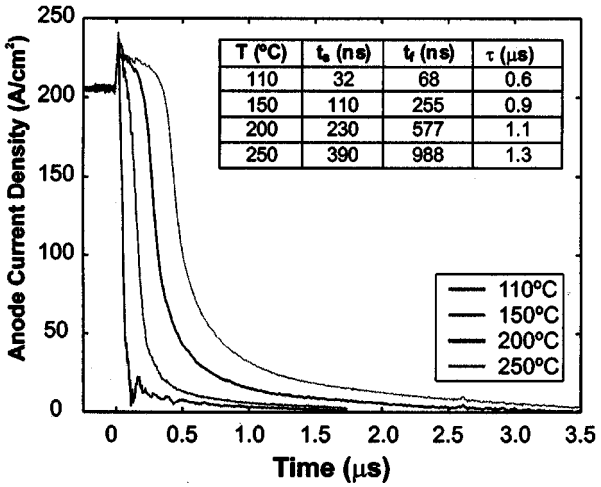

T (°C)	t_s (ns)	t_f (ns)	τ (μs)
110	32	68	0.6
150	110	255	0.9
200	230	577	1.1
250	390	988	1.3

Fig. 9. Turn-off characteristics of an 1100-V 4H–SiC GTO with increasing junction temperature.

parasitic contact resistance on the thyristor forward drop has been quantified [43]. Interestingly, unlike silicon devices, the SiC thyristor turns on faster with increasing temperature because an increase in acceptor activation improves hole injection from the p+ emitters [44], [45]. The turn-off characteristics are shown in Fig. 9 and the turn-off time increases with temperature because of an increase in recombination lifetime. A maximum turn-off current density of over 100 A/cm^2 is possible at 190 °C. The dependence of turn-on and turn-off characteristics on device geometries has also been studied [20]. Furthermore, the turn-off gain of SiC GTO is expected to be less than the silicon counterpart if the complementary structure is adopted. The reason being is that the upper transistor is a p–n–p in the SiC case and, hence, it has less current gain. Experimentally, turn-off gains between three and seven have been measured on 700-V 4H–SiC GTOs [22]. Finally, with the reduced base widths, SiC GTOs can switch at a higher frequency than Si devices of the same rating. For example, 700-V 4H–SiC GTOs with a switching frequency up to 250 kHz have already been reported [22].

D. Materials and Process Challenges

At present, commercial 4H–SiC substrates of up to 3-in diameter are available and custom n- and p-type epitaxial layers up to 50 μm can be ordered. For high-voltage devices, total epitaxial layer thickness of at least up to 30 m with acceptable surface flatness and doping uniformity and minimum compensation is needed. To minimize parasitic substrate resistance and maximize carrier concentration, a substrate resistivity less than 10mΩ-cm would be desired. To achieve that resistivity, however, a carrier concentration of 10^{19} cm^{-3} would be needed and that seems to be difficult with p+ substrates due to the deepness of the acceptor levels (>180 MeV), in addition to the low hole mobility (50 cm^2/V·s). The most severe structural defect is the micropipe, but its density has been substantially improved (to a recently reported value of less than 1 micropipe/cm^2). A defect density of less than 1 micropipe/cm^2 is needed to realize devices of current ratings larger than 100 A with reasonable yield. Other structural defects, such as screw dislocations, appear to correlate with excessive leakage current in 4H–SiC p–n junctions [46]. Despite the continuing improvement of SiC MOS interfacial parameters (to, at present, for 4H–SiC, a fixed oxide charge density close to 10^{12}/cm^2 and an interface state density $\sim 10^{11}$/eV-cm^2 at Ec-E of 0.6 eV [47]–[49]), the correlation between surface state densities with inversion layer mobility is weak. Hence, the inversion layer mobility in 6H- and 4H–SiC needs to be optimized and correlated to surface process conditions.

III. Silicon Carbide Benefits and Advantages for Power Electronic Applications

To show the benefits of SiC for power electronic applications, we first compare a SiC p–i-n diode with state of the art Si diodes from a switching point of view and then we look at the performance of SiC p–i-n diodes in a dc/dc boost converter. We also present the switching characteristics of SiC GTOs, as well as the results from a hybrid single-phase Si/SiC inverter where the modules consist of a Si IGBT in antiparallel with a SiC diode. We also discuss the future of SiC power electronics, potential applications of SiC devices, and major accomplishments in the past five years.

A. DC/DC Converters

1) Background: In most Si-based switching power converter applications, diode reverse recovery switching losses are a significant part of the overall losses. In addition to their inherent losses due to the reverse recovery, diode reverse recovery affects the accompanying switching devices such as IGBTs, MOSFETs, etc., in the form of additional turn-on losses. Other adverse effects of reverse recovery include electromagnetic interference (EMI) and additional thermal management. Silicon diodes have reached their theoretical limits in terms of reverse recovery time. State-of-the-art silicon diodes exhibit reverse recovery times as low as 25 ns for low BVs (<200 V), higher BV diodes (>200 V) exhibit much higher reverse recovery times (35 ns and up) and are inherently much slower (e.g., an ultrafast 400 V, 30 A has a t_{rr} as high as 60 ns). Any reduction in the reverse recovery time would require a drastic improvement of the current technology or a change of the material. Recent progress in SiC material and processing [50] have brought to the market relatively large wafer diameters (50–75 mm) with small micropipe density (<100 cm^{-2}) [51]. In turn, this allows process engineers to build large area devices for power applications.

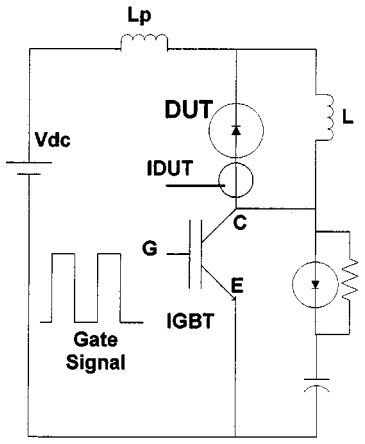

Fig. 10. Reverse recovery test setup.

To show the benefits of SiC- over Si-based devices, we present the results of a comparison between 600-V 50-A ultrafast (HFA50PA60C-trr 25 ns) Si diodes and 4H–SiC diodes with respect to reverse recovery losses [52]. Since these diodes were used in an IGBT boost converter, IGBT turn-on losses were also measured at room temperature (RT) and at 150 °C. The IGBT turn-on losses and diode turn-off losses were measured with the circuit of Fig. 10 in a double-shot mode. The SiC diodes used were still on the wafer and not yet packaged. A probe station is used to connect the SiC diodes to the test circuit. 4H-SiC diodes with a 5-μm drift layer thickness were used. Packaged SiC diodes were also tested using the circuit of Fig. 11 (Boost converter operating in a continuous conduction mode.) Each packaged SiC diode contains two 800-μm × 800-μm dies in a parallel configuration. These diodes were also compared to the previous ultrafast silicon diodes with the same IGBT. In addition to demonstrating the silicon carbide operation in continuous mode at relatively moderate power and at high voltages, this test also allowed for an overall comparison of losses, including conduction losses. Efficiency results were compared for the two cases.

2) Experimental Setup: The SiC diodes were tested directly on the wafer using a probe station according to the circuit of Fig. 10. The diodes were thermally cycled to 150 °C using a thermal chuck. Si diodes were also tested under the same conditions to account for all the circuit parasitics. A fast IGBT is used as the main switch. For each diode, reverse recovery losses, IGBT total turn-on losses as well as IGBT turn-on losses due to diode reverse recovery were measured at 25 °C and 150 °C. With the boost converter circuit of Fig. 11, packaged SiC diodes were tested under light load

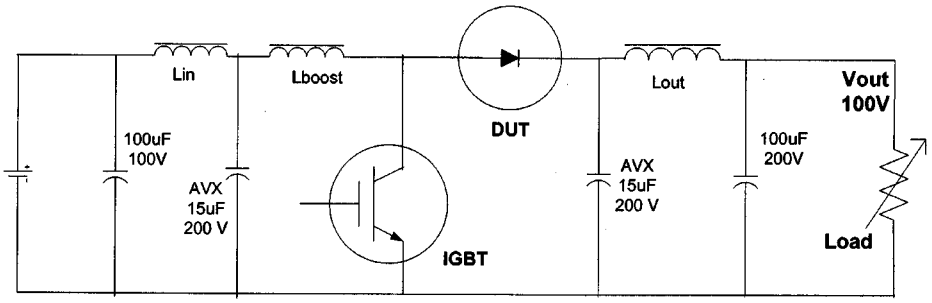

Fig. 11. Hybrid 500-W Si/SiC boost converter.

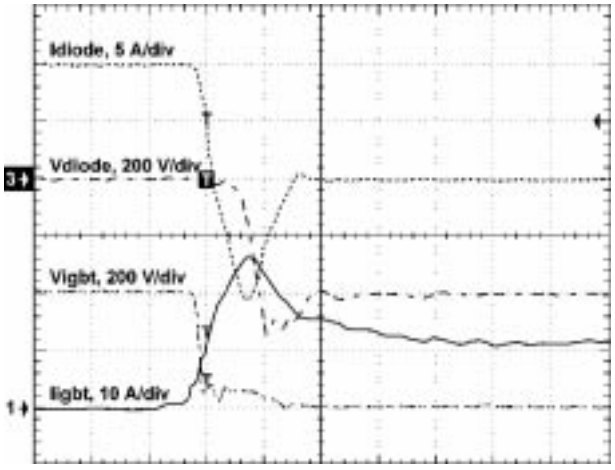

Fig. 12. Voltage and current waveforms at 25 °C when an ultrafast diode is used as DUT, 50 ns/div, $di/dt = 480$ A/μs.

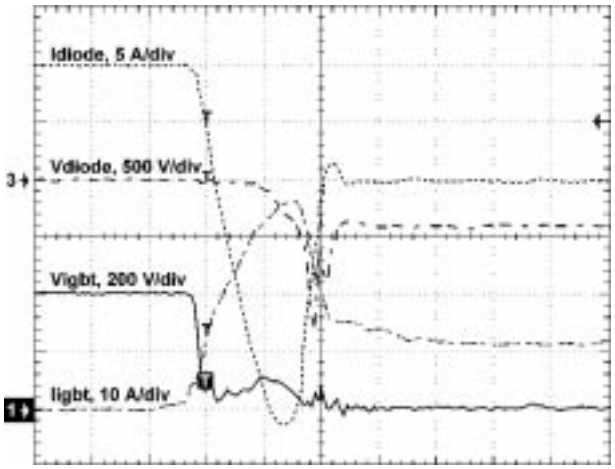

Fig. 13. Voltage and current waveforms at 150 °C when an ultrafast Si diode is used as DUT, 50 ns/div, $di/dt = 480$ A/μs.

(50 W) all the way to full load (500 W). The circuit efficiency with SiC diodes and ultrafast Si diodes was compared.

3) Switching Efficiency:

a) Ultrafast silicon diode: Figs. 12 and 13 show the diode and IGBT voltage and current for a 400-V dc voltage and a 10-A load current. The diode reverse recovery current is on the order of 11 A with a di/dt of 480 A/μs at RT. The reverse recovery time and the reverse peak voltage are on the order of 70 ns and 548 V. The diode recovery losses are

Table 5
Diodes and IGBT Loss Summary Due to Diode Reverse Recovery

	DUT Tj=25°C		DUT Tj=150°C	
	Ultra-Fast Si Diode	*SiC Diode*	*Ultra-Fast Si Diode*	*SiC Diode*
Diode Losses	86μJ	8μJ	268μJ	26μJ
IGBT Losses	88μJ	56μJ	172μJ	56μJ
Total	174μJ	64μJ	440μJ	92μJ

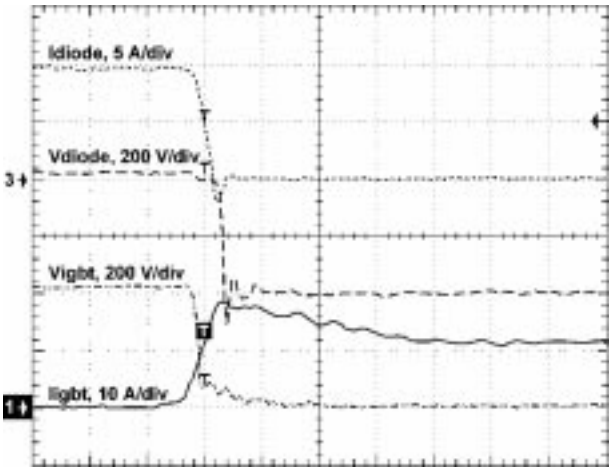

Fig. 14. Voltage and current waveforms at 25 °C when a SiC diode is used as DUT, 50 ns/div, $di/dt = 480$ A/μs.

on the order of 86 μJ. The IGBT turn-on losses are on the order of 136 μJ total with 88 μJ due to diode reverse recovery current only. At 150 °C, the diode reverse recovery current and time increase to 21.4 A and 96 ns, an increase of 100% and 37%, respectively, as shown in Fig. 13. The peak reverse voltage is on the order of 1330 V. The latter is due to the high di/dt at reverse recovery and to the diode "snappiness" at turn-off. The diode and IGBT losses due to diode reverse recovery are 268 μJ and 172 μJ, respectively. These results are summarized in Table 5.

In terms of the forward-biased SOA (FBSOA) of the IGBT, the high voltage seen across the diode and its high reverse recovery current, will push the IGBT into operation at the boundary of the FBSOA.

b) Silicon carbide diode: Figs. 14 and 15 show similar results for a 4H-SiC p–i-n diode. At RT, the very small

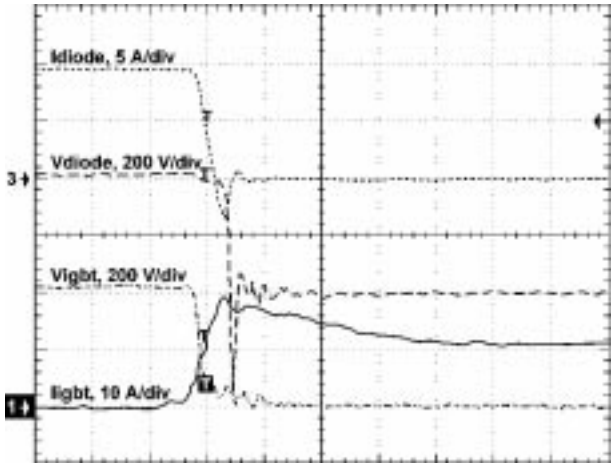

Fig. 15. Voltage and current waveforms at 150 °C when a SiC diode is used as DUT, 50 ns/div, $di/dt = 480$ A/μs.

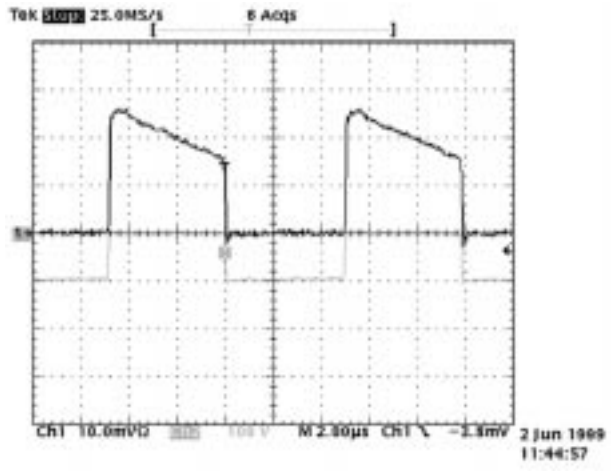

Fig. 16. SiC diode voltage and current at 200-W load, 100-kHz switching frequency, 2 s/div, 2 A/div, 100 V/div. Top: Waveform current. Bottom: Waveform voltage.

reverse recovery time and current of the diode has a tremendous effect on the IGBT turn-on losses, as shown in Fig. 14. As expected, an 80% decrease in reverse recovery current is observed compared to the ultrafast Si diode. The reverse recovery time is reduced by 53 ns (81%) compared to the ultrafast Si diode. Reverse recovery voltage is also reduced by 36 V (7%) compared to the ultrafast Si diode. IGBT turn-on losses due to reverse recovery are reduced by 32 μJ (24%) to 56 μJ compared to the ultrafast Si diode. The diode turn-off loss is only 8 μJ.

At 150 °C, there is an increase in the reverse recovery current from 2.2 A to 3.5 A (60%), but this is still much smaller by orders of magnitude than the ultrafast Si diode results, as shown in Fig. 15. The reverse recovery time increases slightly from 13 ns to 16 ns. The peak reverse voltage increases to about 808 V from 512 V at 25 °C. The IGBT turn-on losses are not affected by the temperature increase in the SiC diode case and remain at 56 μJ, but the SiC diode losses increase slightly to 26 μJ for a total reverse recovery loss of only 92 μJ. These results are summarized in Table 5.

Table 6
Boost Converter Efficiency With Fast, Ultrafast, and SiC Diodes

Target Power	Fast Diode	Ultra-Fast Diode	Silicon Carbide
100W	93.8%	95.5%	93%
200W	93.4%	95.3%	93.4%
300W	92.7%	95.2%	93.3%
400W	92.6%	95.1%	92.9%
500W	92.1%	95.2%	92.1%

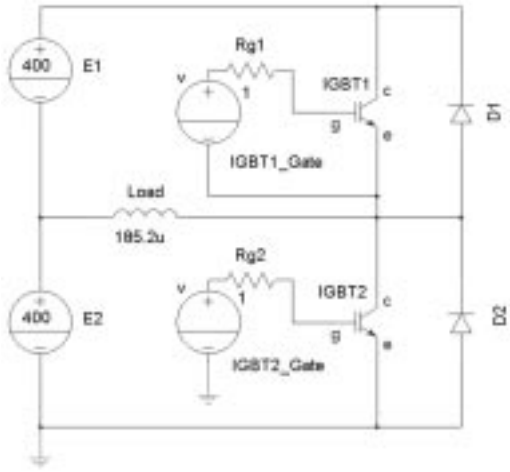

Fig. 17. Single-phase inverter leg simulation model.

c) Converter Efficiency: Silicon carbide diodes packaged in a TO-254 package were used in the boost converter of Fig. 13. Each diode is made with two 800-μm × 800-μm dies in parallel to handle the required current. The converter operates in a continuous conduction mode at 100 kHz switching frequency. Fig. 16 shows the overall switching waveforms of the converter with a silicon carbide diode as a freewheeling diode. These results are for a 500-W output power and for an input voltage of 50 V and an output voltage of 100 V (50% duty cycle). As in the previous case, switching losses are substantially reduced with silicon carbide diodes.

The overall efficiency of the converter is lower with silicon carbide diodes because of the higher SiC conduction losses. These losses are due to the high forward drop of the p–i-n SiC diodes, which is in turn due to the high-energy bandgap (Eg) of SiC and to the high series resistance. In our case, the SiC diodes have a forward drop as much as 3–4 V at 2.5 A. With SiC Schottky diodes, this forward drop can be expected to be on the order of 1.5–2-V maximum, hence, making SiC Schottky diodes more attractive and more competitive with their Si counterpart. Recent commercial Schottky diodes rated at 600 V and 6 A exhibit forward drops of 1.5–2.1-V max [53]. A summary of the efficiency results is shown in Table 6. At higher BVs, it is expected that SiC benefits will improve due to low forward voltage drops and higher current densities. At voltages higher than 5 kV, SiC p–i-n diodes will outperform their Si counterpart both for conduction and switching losses.

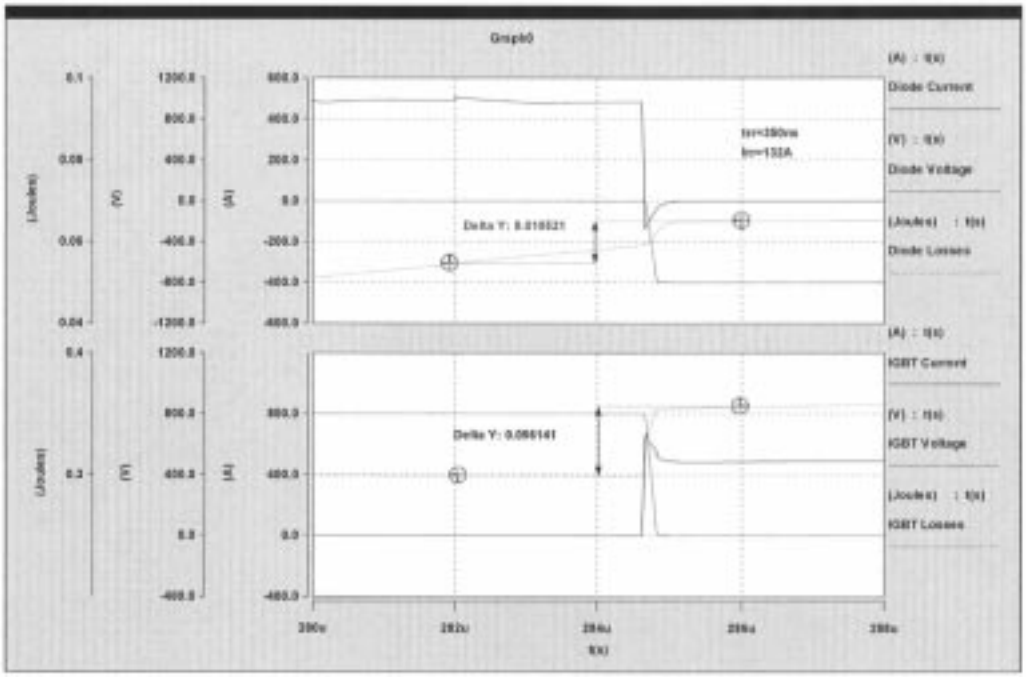

Fig. 18. Ultrafast silicon diode as flyback diode. Moderate losses, moderate stress on IGBTs.

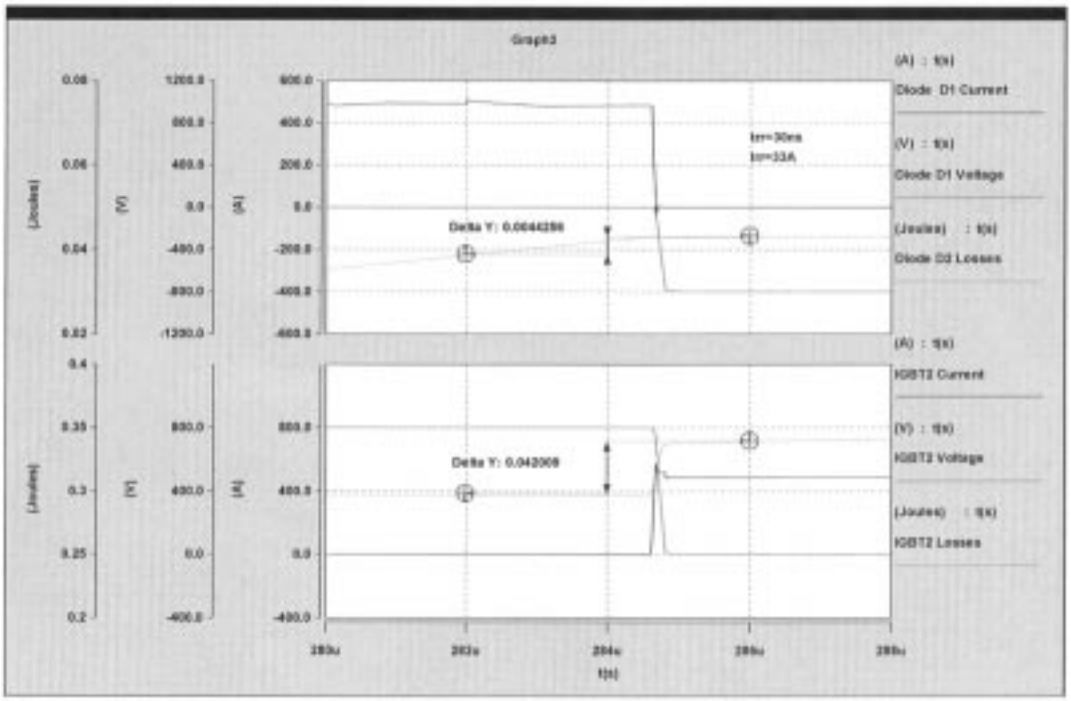

Fig. 19. Ultrafast silicon diode as flyback diode. Low losses, low stress on IGBTs.

B. DC/AC Converters: Hybrid Si/SiC Applications

1) Single-Phase Inverter Leg Simulation: To quantify the benefits of SiC over Si-based devices, simulations of a single-phase inverter leg were performed, where the antiparallel diodes are either ultrafast silicon or silicon carbide. Fig. 17 shows the schematic of a half-bridge phase leg inverter used in the simulation, driving an inductive load from a split dc supply. This bridge type serves as a building block for most high-power conversion applications. In this model, the active switches are silicon-based IGBTs. For this application a major concern is the effect of reverse recovery

Table 7
Comparison of Simulated Reverse Recovery Losses of 1200-V 600-A Ultrafast Si Versus SiC Diode

	Ultra-Fast Si Diode	SiC Diode
Diode Reverse Recovery Losses	12 mJ	1mJ
Switch Turn-on loss from RR	13 mJ	2 mJ
Total Losses from Reverse Recovery	**25 mJ**	**3 mJ**
% Reduction	-	88% !!

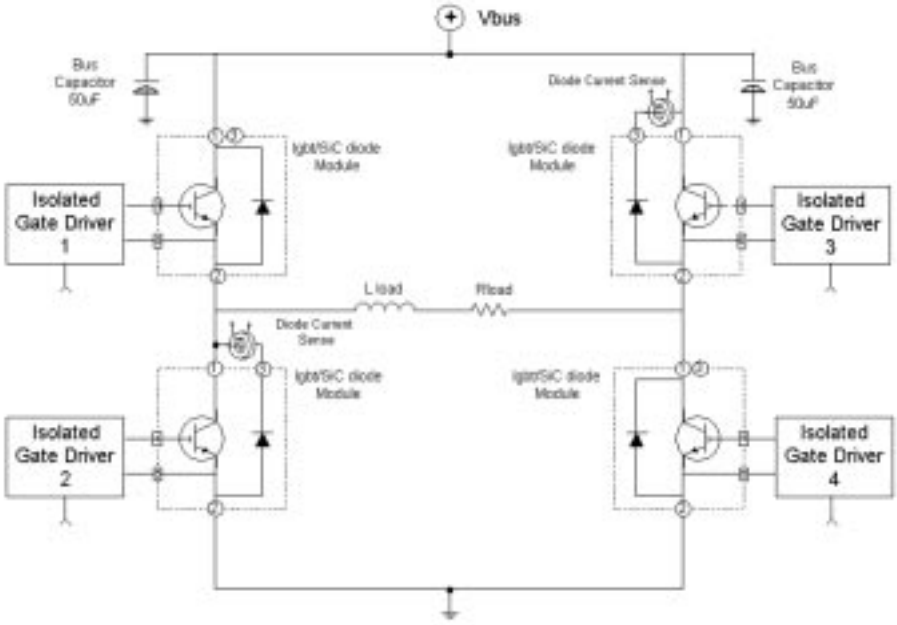

Fig. 20. Schematic of full-bridge PWM inverter.

of diode D2 on the turn on of IGBT1 and diode D1 on the turn-on of IGBT2. The higher reverse recovery current and time associated with silicon diodes translate into higher current stress, and hence higher switching losses, on the IGBTs during the turn-on transition. Fig. 18 shows IGBT1 and diode D2 voltage and current waveforms as well as IGBT1 turn-on switching losses when an ultrafast Si diode is used as the antiparallel diode D2. Note the high reverse recovery current and time associated with the Si diode. In this example, the dc bus is 800 Vdc and the load current is 500-A peak. The diode reverse recovery current is on the order of 130 A or ∼25% of the peak load current. This recovery current is superimposed on the peak load current resulting in a peak current stress in the IGBT on the order of ∼630 A. Moreover, this additional current stress in the IGBT also induces higher switching losses on the order of 56 mJ of which 14 mJ is strictly due to the diode reverse recovery. In addition to the increased losses in the IGBT, the reverse recovery losses in the diode itself is ∼11 mJ, making the total losses due to the relatively poor reverse recovery of Si-based diodes on the order of 25 mJ or 500 W at 20 kHz.

For the above example with the Si diode replaced by an equivalent SiC diode with the resulting waveforms shown in Fig. 19, the reverse recovery current at turn-off of the diode D2 is dramatically reduced to 33 A or ∼75% reduction, while the reverse recovery time is reduced by ∼90%. This in turn substantially reduces the diode reverse recovery losses to <1 mJ and, consequently, the IGBT1 total turn-on losses to about 42 mJ or 20% reduction compared to Si-based diodes. The total losses due to one diode turn-off event are <3 mJ or 60 W at 20 kHz, a reduction of 90% compared to the fastest Si-based diodes. From the above analysis, it is seen that with SiC devices, in general, designers now have an opportunity to reduce system size and weight by reducing thermal management requirements. Power semiconductor devices can now be operated at much higher junction temperatures allowing for operation at much higher switching frequencies and in very harsh environments. The latter will be made possible by the future availability of SiC switches and diodes at the commercial level.

Table 7 summarizes the comparative results between an ultrafast Si diode and a SiC diode. The results shown in this table are based on the single-phase inverter simulation shown above. These results are corroborated with experimental data (see Figs. 14 and 15) obtained from a lot of SiC p–i-n diodes fabricated at GE under the Defense Advanced Research Projects Agency SiC Megawatt Program MDA972-98-C-0001. The reverse recovery current (Irr) was reduced by almost 86% (from 21 A to 3 A) and the transient reverse recovery time (trr) was reduced by 84% (from 96 ns to 16 ns). With this dramatic reduction in trr and Irr, the total switching losses are substantially reduced allowing SiC-based converters to operate at much higher switching frequencies and much higher junction temperatures.

2) Hybrid Single-Phase 1-kW Si/SiC Inverter: Fig. 20 shows a hybrid Si/SiC inverter where the traditional silicon antiparallel diodes are replaced by SiC p–i-n diodes. Schottky SiC diodes can also be used in this application to replace the Si diodes. With Schottky diodes, the designer has a chance to closely match the forward drop of the Si diodes. With low to medium voltage (up to 3000 V) SiC p–i-n diodes, the forward drop is inherently larger than for a similar Si diode because of the larger SiC bandgap. For this particular application, we constructed hybrid modules as shown in Fig. 21 out of 600-V 75-A Si IGBT chips and 6 × 600-V 3-A SiC p–i-n diodes connected in antiparallel. The SiC dies measure 800 μm × 800 μm and were built on 5-μm-thick epi. Two versions of the module were developed,

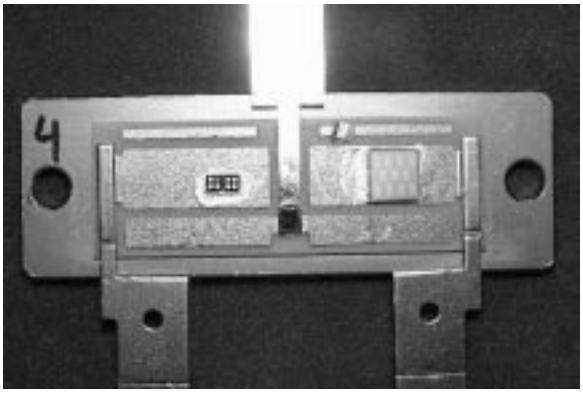

Fig. 21. Integrated module after die attach.

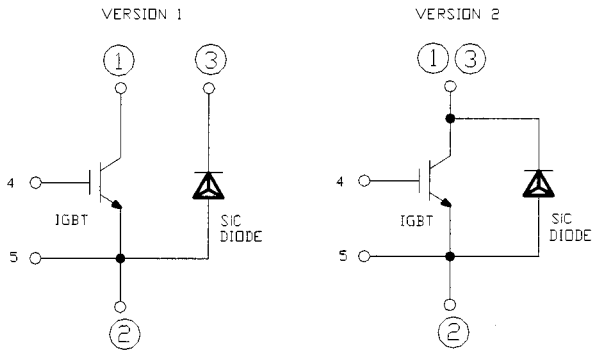

Fig. 22. Integrated module circuit diagram.

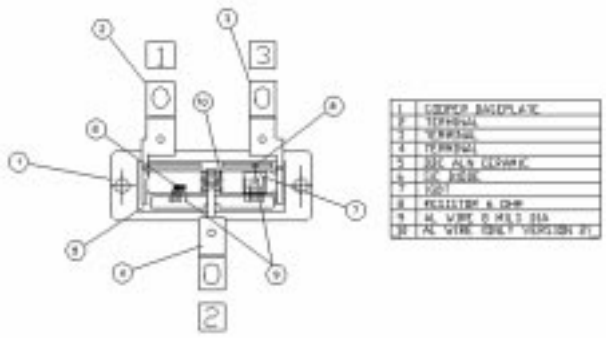

Fig. 23. Assembly elements of integrated module.

as shown in Fig. 22. In version 1, the Si IGBT collector is connected to a separate terminal from the SiC cathode to give the designer more flexibility. For instance, this configuration allows the insertion of a current measuring device in series with either the IGBT or the diode. In version 2, these terminals are hardwired together inside the package, although for facilitating external wiring terminals 1 and 3 are two physically different terminals located on opposite sides of terminal 2 in the package. Fig. 23 shows a drawing of the element assembly with a corresponding list of the main items. An AlN ceramic layer is directly bonded to a copper base plate, which forms the mechanical support of the package. The SiC diode is located on the left-hand side, while the Si IGBT is on the right-hand side. They are die-attached to separate metal-plated pads, which extend to terminals 1 and 3, respectively. In version 2, these pads are shorted together by Al wires, as explained earlier.

Table 8
Hybrid Si/SiC Efficiency Test Results

DC Bus Voltage	100V	150V	200V	250V
Load Input Power	114W	250W	440W	690W
Hybrid Si/SiC Efficiency	**90.6%**	**96.3%**	**97.5%**	**97.8%**
All Si Inverter Efficiency	**92%**	**92.7%**	**95.5%**	**97.1%**

A hard-switched pulsewidth-modulated (PWM) single-phase full-bridge inverter was built using four integrated hybrid Si/SiC modules. The PWM switching frequency is set to 20 kHz, while the signal frequency is set to 2 kHz. An all Si Inverter was also built to serve as a baseline for efficiency and switching loss comparison. Efficiency measurements were performed on both inverters and are shown in Table 8. At light load, the high forward drop of the SiC diode increases the conduction losses and therefore reduces the inverter efficiency. As the load current increases, switching losses become dominant and SiC diodes have an edge over Si diodes. As the load current increases again, the conduction losses become dominant again and the all Si inverter efficiency is as good as the hybrid Si/SiC inverter. Silicon carbide benefits would have been more evident at high switching frequency operation and with high dc bus voltages. Using SiC Schottky diodes rather than p–i-n diodes would also have contributed to an improvement in the hybrid Si/SiC inverter efficiency [54].

C. Other Applications

The results presented on the dc/dc and dc/ac converters demonstrate the advantages of using SiC devices in power converters. In addition to providing low switching losses, low voltage, and current stress, SiC devices can operate at much higher junction temperatures. They also are able to operate at very high voltages and very high switching frequencies. The benefits for circuit designers are tremendous, especially for applications that require high voltages such as X-ray tubes, high temperature such as aircraft engines power supplies, and high switching frequency such as high power-density converters. SiC diodes can also be used in hybrid applications such as drive systems. The low switching losses, low reverse recovery current, and time will allow power converters to operate at high efficiency and low EMI [55]–[57].

With all the advantages that SiC offers, it is not hard to find applications that can benefit tremendously from SiC properties. Such applications are found in various industries such as medical systems, lighting systems, aerospace and aviation systems. With the continuous improvement in the quality of the starting material and with better lifetime control techniques, low forward drop SiC devices will soon be available to the general public [58], [59]. In the following sections, we

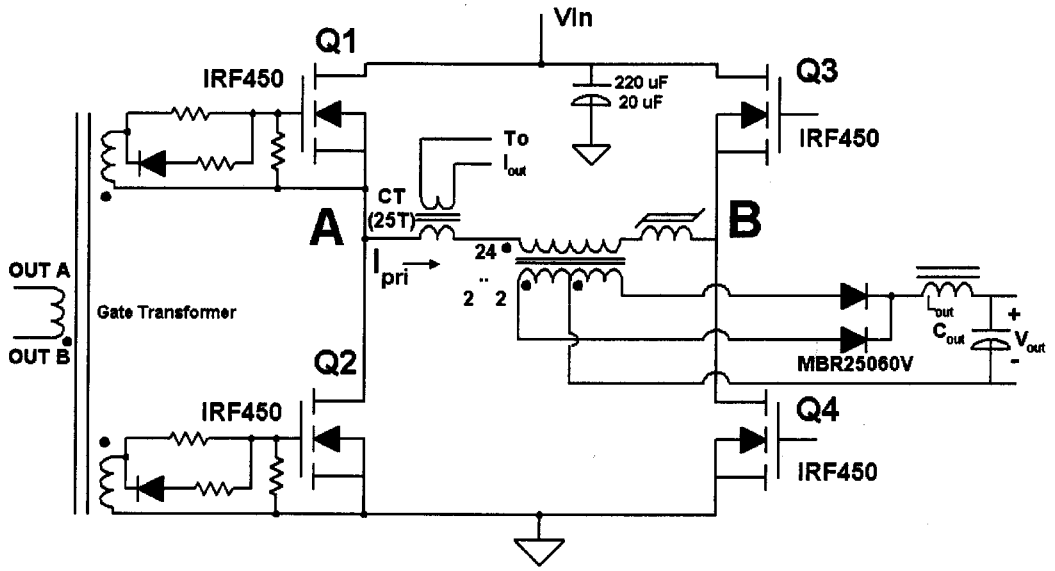

Fig. 24. Circuit topology of high-density converter.

will review some of these applications and also show the benefits of other SiC devices such as BJTs and GTOs. Although most of these devices are still in their infancy, early prototypes are showing a lot of promise [20], [21], [60], [61].

1) High Power-Density Converters: For high power-density power supplies, the main requirements are high efficiency and high density to minimize power loss and space allocated for the converter. Although these parameters depend on both the active and passive components, their values are mainly dependent on the frequency and temperature capabilities of the power devices because in Si they are the most stringent among the circuit components [56]. As discussed in the previous sections, SiC power devices lift these limitations allowing up to ten times higher frequency operation with low switching losses in the megahertz range and, in addition, higher junction temperature in the 200 °C –300 °C regime. Several key benefits result from this change. First, a high frequency design allows reducing the size of inductors and capacitors for a given power rating, thereby increasing the converter power density. Second, the combined effect of higher junction temperature and lower switching losses results in higher power efficiency because less power is dissipated and it is disposed of at higher rate due to the increased thermal difference between heat source and sink. Simulations have predicted a 50% power density improvement for a 100-V 2-kV dc–dc boost converter by replacing Si with SiC [56]. The assumptions included a frequency change from 50 kHz to 500 kHz and a junction temperature change from 150 °C to 300 °C. The corresponding power density increased from 4 W/cm^3 to 7 W/cm^3 and the converter efficiency from 85% to 89% [56].

Fig. 24 shows a low-noise high-density 1-kW 270-V dc to 10-V dc output 250-kHz switching frequency power converter for avionic applications. This basic converter uses a full-bridge edge-resonant PWM converter topology. It uses Si Schottky diodes at the secondary of the transformer for rectification. The Si diode junction capacitance rings with the transformer leakage inductance, causing EMI, overvoltages, and stress on other components and limiting switching frequency [62], [63]. The transition to SiC diodes will enable a solution to this problem because of the low reverse recovery time and small junction capacitance. SiC diodes have a low junction capacitance compared to Si diodes. The junction capacitance measurement results from a 600-V 25-A SiC diode and a 600-V 25-A Si diodes show a reduction of the capacitance from 540 pF at zero voltage bias for Si diodes to 17 pF for SiC diodes. At higher voltages (400 V), the capacitance decreases from 20 pF (Si) to 4pF (SiC). This reduction in the junction capacitance is due to the smaller area required by SiC diodes compared to Si diodes for the same current and voltage ratings. In addition to reducing the noise due to the ringing effect, SiC diodes will also allow an improvement in the overall efficiency through switching loss reduction. Since SiC Schottky diodes are capable of operating at much higher voltages than their Si counterpart, this particular design can benefit from this feature by reducing the size of the transformer and allowing for high output voltage power supplies.

2) High-Voltage Resonant Converters: Another application where SiC diodes will have a large impact is high-voltage X-ray generator power supplies shown in Fig. 25. These power supplies require very high voltage (up to 150 kV), low current (1.5-A average), and fast diodes at the transformer secondary [64]. The lack of adequate high voltage Si diodes that meet these requirements lead designers to connect in series as many as 25 1-kV diodes per module and then connect in series-six modules to achieve the 150-kV requirement. High-voltage silicon diodes are available up to 10 kV, but their forward voltage drop is exorbitant, i.e., for a 10-kV diode, forward voltage drop is as high as 50 V at 1 A [65]. The high reverse recovery current and time of high-voltage silicon diodes adds to the complexity and low efficiency of these systems. High-voltage silicon

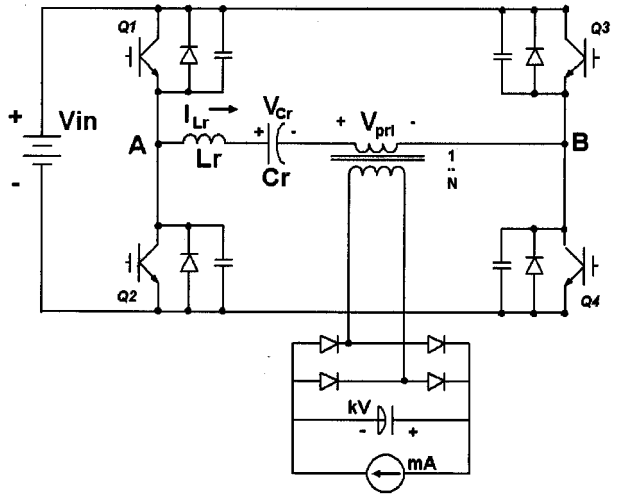

Fig. 25. X-ray generator resonant power supply.

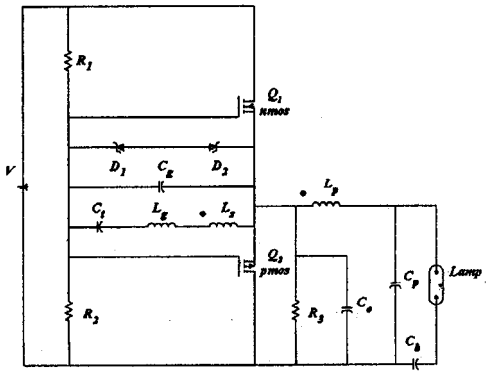

Fig. 26. Typical lighting ballast resonant converter.

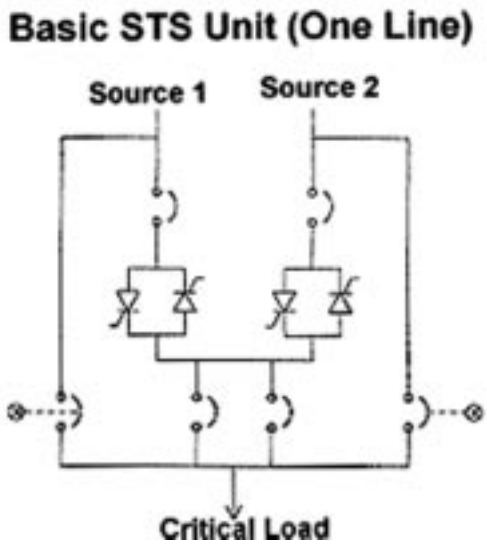

Fig. 27. One-line static transfer switch configuration.

carbide p–i-n diodes with ratings up to 12 kV have been reported [66]. A 12-kV SiC p–i-n diode would require only 120 μm epitaxial layer thickness as opposed to 1200 μm for a similar Si diode. A 150-kV diode would require only 15 diodes in series instead of the 150 $\times$ 1-kV Si diodes. The overall forward drop of a 150-kV SiC p–i-n diode will be an order of magnitude smaller than its Si counterpart. In addition, the low reverse recovery characteristics of the SiC p–i-n diodes will allow these converters to operate at a much higher switching frequency at the primary side. Further, if the primary IGBT modules were replaced by hybrid Si IGBT/SiC Schottky modules, the overall gain in the efficiency will be substantial.

3) Low-Voltage High-Temperature Applications: There are several low-voltage applications where high temperature operation is required. In avionic applications, power supplies are used in harsh environment where the ambient temperature can well exceed the current limit of Si devices [67], [68]. In lighting applications, new compact designs require the integration of the ballast and the lamp in a single package. Such arrangement will lead to higher junction temperature for the ballast switching devices. Similarly in avionic applications, placing power supplies close to the engine will expose the switching components to higher ambient temperature. Both of these applications currently use low voltage (100–600 V) devices such as Schottky diodes, power MOSFETs, BJTs, and in some cases IGBTs. We discussed in the previous sections the SiC Schottky diodes and mentioned that these devices are currently available at the 100–600-V voltage level. Power MOSFETs, BJTs, and IGBTs are still in the development stage and are still facing multiple hurdles and challenges such as low channel mobility for MOSFETs and IGBTs and lack of experience with SiC BJTs.

Fig. 26 shows a typical resonant converter used in lighting applications. When this converter is integrated with the lamp, all of its parts are subject to high temperature. In a typical 20-W 120-V halogen ballast, temperatures can go as high as 230 °C. With the use of SiC devices, the switching devices' temperature is no longer a problem and higher wattage lamp can be integrated with their ballasts. In addition to the switching devices, other devices such as capacitors, transformers need to also sustain high temperatures. Since SiC FETs are still suffering from low channel mobility, SiC BJTs are becoming potential candidates for high-temperature low-voltage applications. Recently, an 1800-V 4-A BJT with a gain of 20 have been reported [69]. A combination of a SiC BJT and a Schottky diode can benefit a number of lighting applications and other high temperature and harsh environment applications such as sensors and avionic products [70]. In these applications, semiconductor devices are required to operate at junction temperatures as high as 750 °C. In a typical avionic application, the use of SiC-based electronics would save a substantial amount of wiring and connectors, hence improving the overall system reliability [71].

4) Power System Applications: High-voltage high-current semiconductor devices such as diodes, GTOs, and thyristors have been used in power system applications for over three decades. Applications such as static volt ampere reactive (VAR) compensators, static transfer switches, dynamic voltage restorers/regulators, electronic tap changers, high-voltage dc transmission systems, and flexible ac

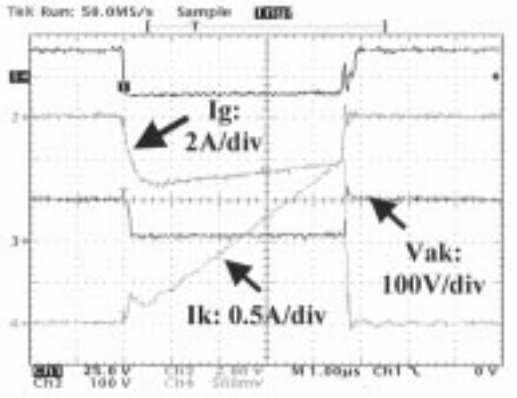

(a)

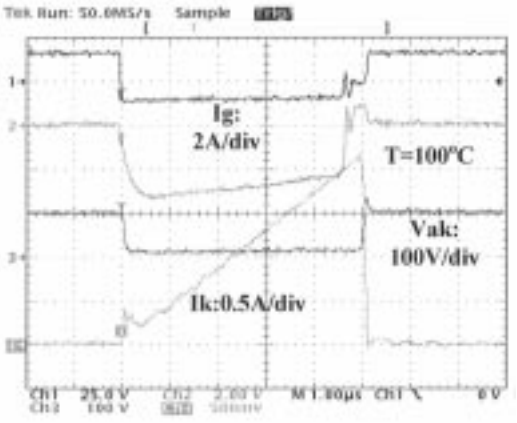

(b)

Fig. 28. (a) SiC GTO on-wafer switching waveforms at RT. (b) SiC GTO on-wafer switching waveforms at 100 °C.

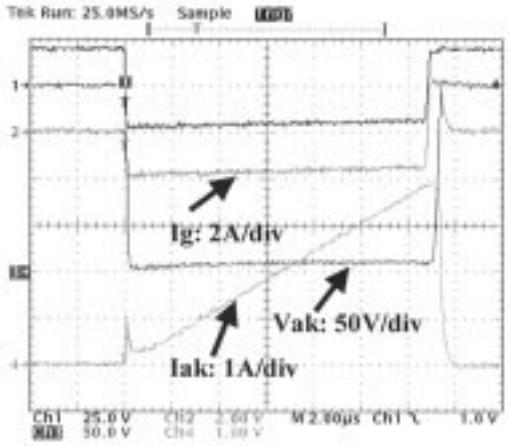

(a)

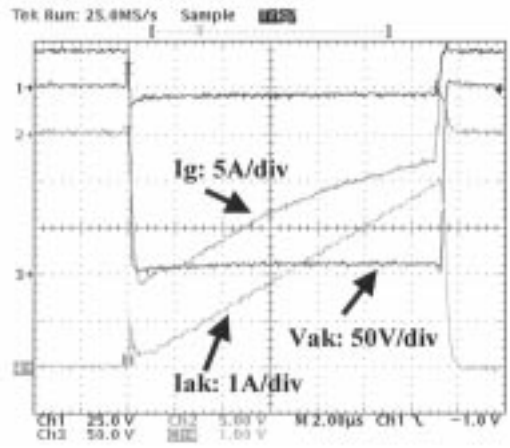

(b)

Fig. 29. (a) Soft-driven packaged SiC GTO switching waveforms at RT. (b) Hard-driven packaged SiC GTO switching waveforms at RT.

transmission lines [5]–[8] all use power devices such as thyristors, GTOs, and diodes. In a typical transfer switch as shown in Fig. 27, thyristors with voltage ratings up to 25 kV and current handling up to 5000 A are needed for medium voltage transfer switches. The current state of the art in Si allows for a maximum of 6–10 kV and currents up to 5000 A. System designers use multiple devices in series and parallel to achieve the required voltage and current ratings. When devices are used in series and parallel, designers need to ensure that they share voltage and current equally; hence, more passive devices such as balancing resistors, capacitors, and even active/passive snubbers are often used. The latter add more weight and increase the size and complexity of these already complicated systems. SiC devices can greatly simplify the design of this equipment by providing high-voltage and high-current devices, hence, reducing the overall number of devices and leading to reduced system size, complexity, and enhanced reliability. The high junction temperature operation of SiC devices will further reduce the size of these systems by requiring less cooling and smaller heat sinks [73].

Prototype high-voltage SiC thyristors and GTOs are rated up to 3-kV BV with 10-A current carrying capability [20], [21]. Although these devices are still small compared to their Si counterparts, their capability and advantages are much superior. As the material quality improves, large area devices; hence, large current carrying devices will be available. Fig. 28(a) and (b) shows the GTO switching waveforms at RT and 100 °C for a 1200-μm diameter 12-μm epi involute gate unpackaged GTO. The devices are hard driven with a high gate current at turn-on. At turn-off, the gate current is on the order of 680 mA at RT and increases to 920 mA at 100 °C for a load current of 4A. In terms of gain, the GTO gain at turn-off is on the order of five to seven (a higher than typical value compared to Si GTOs) at RT and decreases to four (a typical value for Si GTOs) at 100 °C. Turn-off time is on the order of 600 ns at RT and increases to 720 ns at 100 °C. These turn-off times are much lower than similar values for silicon devices. Although Si GTOs are not available at these sizes for a direct comparison, it is conceivable that SiC GTOs will remain much faster than similar GTOs even at high-current ratings because of the intrinsic properties of SiC. Fig. 29(a) and (b) shows 200-V 4-A switching waveforms of packaged GTOs. In Fig. 29(a), the devices are soft driven using a series resistance in the gate circuit to lower the gate current required to turn on the devices. In Fig. 29(b), the devices are hard driven and a much higher gate current is required to turn-on the devices. The gain at turn-off remains the same (on the order of two). These devices exhibit a very fast turn-on and

turn-off. The results presented so far show that SiC GTOs will potentially be viable in the next three to five years as the material quality improves and larger wafer diameters are produced [61]. The devices presented here are of limited size due to the large defect densities still present in SiC; however, with the steady progress in SiC material growth made over the past ten years, material quality appears to be a technological rather than a fundamental barrier [14]–[16].

5) Pulse-Power Applications: Pulse-power applications represent another promising area where SiC devices can play an important role in providing the devices that will meet the stringent requirements of pulse-power applications, such as high-energy military applications [74]–[77]. A typical pulse-power device is required to handle tens if not hundreds of thousands of amps, sustain a high BV, and be able to stand a very high di/dt (>10 kA/μs) within a short amount of time on the order of sub microseconds to 100 μs [78]–[82]. The devices are also required to stand very high junction temperature without going into self-destruction or thermal run away. Pulse-power designers are currently using either vacuum technology for very high-voltage applications [82] or high-voltage pulse SCRs rated at 5 kV and capable of peak currents on the order of 250 kA [81]. These devices are limited in term of switching frequency and their recovery times prohibit multiple pulse applications. Multiple pulse applications, where devices are pulsed a number of times in a short interval, are required in some applications such as the electromagnetic gun. This need arises either to fulfill the mission specifications or to reduce the overall system size by taking advantage of new advanced electrical machines concepts.

SiC devices will allow the use of high-voltage devices, capable of high di/dts and with fast turn-on and turn-off capability [77]. The SiC high power density will allow designers to reduce the size of the overall system by requiring a small number of devices to accomplish the high peak current requirement. The high junction temperature and improved thermal performance of SiC will reduce the size of the cooling system and will lead to substantial savings of size and weight, especially for advanced applications such as combat vehicles where size and weight are a premium. Studies have estimated that a silicon carbide pulse-power system will require only 40% of the volume and weight of a Si-based system [77]. With high current density beyond 6 kA/cm^2 and di/dts improved by a factor of three to five over Si, SiC devices can significantly enhance the performance of pulse-power equipment and allow designers more flexibility in the design of other components such as the power source.

IV. Summary and Conclusion

The future of SiC power devices appears bright. The continued reduction of defect density, including micropipes, and the increase of wafer diameter are two important factors for increasing the chip size and consequently the current rating. The increase of epitaxial layer thickness for both n- and p-type lightly doped layers will lead to higher voltage rating for p–i-n diodes and GTOs. As wafers with higher carrier lifetime become available, it is expected that carrier lifetime control will be used, as done for Si. Process technology will further evolve and adjust to the transition from the device demonstration phase to the manufacturing phase with increased attention being devoted to yield improvement and SiC manufacturing efficiency.

Although the advantages of SiC over Si are well known, the transition to SiC commercial devices will take some time, but it will ultimately revolutionize power electronics by allowing high temperature, very high switching frequency, and very high-voltage operation. High-temperature operation will permit operation in much harsher environments such as avionics where converters can be subjected to higher ambient temperatures. Higher switching frequencies will lead to substantial reduction of size and weight, hence, contributing to lower cost and higher portability. Higher voltages will enable the use of fewer devices (in series) in high-voltage applications such as X-ray generators and power systems converters.

Acknowledgment

The authors would like to thank D. Radack of DARPA MTO and G. Campisi of ONR for their support. The authors would also like to thank the following individuals whose help and support made this paper possible: M. Ghezzo, S. Arthur, M. Kheraluwala, M. Schutten, J. Fedison, J. Park, J. Kretchmer, A. W. Clock, R. Steigerwald, M. Lazzeri, P. Gipp, D. Herbs, E. Jacobson, M. Gibeau, G. Croff, all of GE Corporate Research and Development. They would also like to thank V. Khemka of Motorola and N. Ramungul of the Thai Industrial Standards Institute, Thailand, for their contributions to the SiC effort at GE and RPI. The authors would like to thank the anonymous reviewers for their valuable and insightful comments.

References

[1] S. Bernet, "Recent developments of high power converters for industry and traction applications," *IEEE Trans. Power Electron.*, vol. 15, pp. 1102–1117, Nov. 2000.

[2] H. Yilmaz, Owyang, M. F. Chang, J. L. Benjamin, and W. R. Van Dell, "Recent advances in insulated gate bipolar transistor technology," *IEEE Trans. Ind. Applicat.*, vol. 26, pp. 831–834, Sept.–Oct. 1990.

[3] B. P. Muni, A. V. Gokuli, and S. N. Saxena, "Gating and protection of IGBT in an inverter," in *Proc. Int. Conf. Industrial Electronics, Control, and Instrumentation*, vol. 1, 1991, pp. 662–667.

[4] A. Petterteig, J. Lode, and T. M. Undeland, "IGBT turn-off losses for hard switching and with capacitive snubbers," in *Proc. IEEE Industry Applications Society Annu. Meeting*, vol. 2, 1991, pp. 1501–1507.

[5] N. Hingorani, "Introducing custom power," *IEEE Spectrum*, vol. 32, pp. 41–48, June 1995.

[6] ——, "Flexible ac transmission," *IEEE Spectrum*, vol. 30, pp. 40–45, Apr. 1993.

[7] F. Nozari and H. S. Patel, "Power electronics in electric utilities: HVDC Power Transmission Systems," *Proc. IEEE*, vol. 76, pp. 495–506, Apr. 1988.

[8] L. Gyugyi, "Power electronics in electric utilities: Static Var Compensators," in *Proc. IEEE*, vol. 76, Apr. 1988, pp. 483–494.

[9] M. Morikawa, K. Nakura, M. Ito, N. Machida, S. Yamada, S. Kudo, S. Shimizu, and I. Yoshida, "Highly efficient 2.2-GHz Si power MOSFETs for cellular base station applications," in *Proc. IEEE Radio and Wireless Conf.*, 1999, pp. 305–307.

[10] T. W. Ching, K. T. Chau, and C. C. Chan, "A novel zero-voltage soft-switching converter for switched reluctance motor drives," in *Proc. 24th Annu. IEEE Industrial Electronics Society Conf.*, vol. 2, 1998, pp. 899–904.
[11] J. Blanc, "Practical application of MOSFET synchronous rectifiers," in *Proc. 13th Int. Conf. Telecommunications Energy*, Nov. 1991, pp. 495–501.
[12] L. Lorenz, G. Deboy, A. Knapp, and M. Marz, "COOLMOS/sup TM/-a new milestone in high voltage power MOS," in *Proc. 11th Int. Symp. Power Semiconductor Devices and ICs*, 1999, pp. 3–10.
[13] C. M. Johnson, N. G. Wright, S. Ortolland, D. Morrison, K. Adachi, and A. O. O'Neill, "Silicon carbide power devices: Hopeful or hopeless?," in *Proc. IEE Colloq. Recent Advances in Power Devices*, 1999, pp. 10/1–10/5.
[14] H. Matsunami, "Progress in wide bandgap semiconductor SiC for power devices," in *Proc. 12th Int. Symp. Power Semiconductor Devices and ICs*, 2000, pp. 3–9.
[15] G. J. Campisi, "Status of silicon carbide power technology," in *Proc. Power Engineering Society Summer Meeting*, vol. 2, July 2000, pp. 1238–1239.
[16] J. W. Palmour, R. Singh, R. C. Glass, O. Kordina, and C. H. Carter, "Silicon carbide for power devices," in *Proc. 9th Int. Symp. Power Semiconductor Devices and ICs*, 1997, pp. 25–32.
[17] B. J. Baliga, "Power semiconductor device figure of merit for high-frequency applications," *IEEE Electron Device Lett.*, vol. 10, pp. 455–457, Oct. 1989.
[18] Cree, Inc. Announces Introduction and Availability of 3 Inch 4H SiC Wafers [Online]. Available: http://www.compoundsemiconductor.net
[19] Infineon Technologies Produces World's First Power Semiconductors in Silicon Carbide [Online]. Available: http://www.compoundsemiconductor.net
[20] J. B. Fedison, T. P. Chow, A. K. Agarwal, S. H. Ryu, R. Singh, O. Kordina, and J. W. Palmour, "Switching characteristics of 3 kV 4H–SiC GTO thyristors," in *Proc. 58th Annu. Device Research Conf.*, 2000, pp. 135–136.
[21] S. H. Ryu, A. K. Agarwal, R. Singh, and J. W. Palmour, "3100V asymmetrical, gate turn-off thyristors in 4H–SiC," *IEEE Electron Device Lett.*, vol. 22, pp. 127–129, Mar. 2001.
[22] S. Seshadri, J. B. Casady, A. K. Agarwal, R. R. Siergiej, L. B. Rowland, P. A. Sanger, C. D. Brandt, J. Barrow, D. Piccone, R. Rodrigues, and T. Hansen, "turn-off characteristics of 1000 V SiC gate-turn-off thyristors," in *Proc. 10th Int. Symp. Power Semiconductor Devices and ICs*, 1998, pp. 131–134.
[23] K. Chatty, T. P. Chow, R. J. Gutmann, E. Arnold, and D. Alok, "Accumulation-layer electron mobility in n-channel 4H–SiC MOSFETs," *IEEE Electron Device Lett.*, vol. 22, pp. 212–214, May 2001.
[24] R. Singh, K. G. Irvine, O. Kordina, J. W. Palmour, M. E. Levinshtein, and S. L. Rumyanetsev, "4H–SiC bipolar P-i-N Diodes with 5.5 KV blocking voltage," in *Proc. 56th Annu. Device Research Conf.*, 1998, pp. 86–87.
[25] K. Shenai, R. S. Scott, and B. J. Baliga, "Optimum semiconductors for high power electronics," *IEEE Trans. Electron Devices*, vol. 36, pp. 1811–1823, Sept. 1989.
[26] A. Bhalla and T. P. Chow, "Examination of semiconductors for bipolar power devices," *Proc. Inst. Phys. Conf.*, no. 137, p. 621, 1994.
[27] A. Bhalla and T. P. Chow, "Bipolar power device performance: dependence on materials, lifetime and device ratings," in *Proc. 6th Int. Symp. Power Semiconductor Devices and ICs*, 1994, pp. 287–292.
[28] T. P. Chow and R. Tyagi, "Wide bandgap compound semiconductors for superior high-voltage power devices," *IEEE Trans. Electron Devices*, vol. 41, pp. 1481–1482, 1994.
[29] B. J. Baliga, *Power Semiconductor Devices*. Boston, MA: PWS Publishing, 1996.
[30] S. K. Ghandhi, *Semiconductor Power Devices*. New York: Wiley, 1977.
[31] M. Bhatnagar, P. K. McLarty, and B. J. Baliga, "Silicon carbide high-voltage (400V) Schottky barrier diodes," *IEEE Electron Device Lett.*, vol. 13, pp. 501–503, Oct. 1992.
[32] R. Raghunathan, D. Alok, and B. J. Baliga, "High voltage 4H–SiC Schottky barrier diodes," *IEEE Electron Device Lett.*, vol. 16, pp. 226–228, June 1995.
[33] A. Itoh, T. Kimoto, and H. Matsunami, "Low power-loss 4H–SiC Schottky rectifiers with high blocking voltage," in *Proc. Inst. Phys. Conf.*, 1995, pp. 689–692.
[34] K. Ueno, T. Urushidani, K. Hashimoto, and Y. Seki, "The guard-ring termination for the high-voltage SiC Schottky barrier diodes," *IEEE Electron Device Lett.*, vol. 16, pp. 331–332, July 1995.
[35] C. E. Weitzel, J. W. Palmour, C. H. Carter Jr, K. Moore, K. J. Nordquist, S. Allen, C. Thero, and M. Bhatnagar, "Silicon carbide high power devices," *IEEE Trans. Electron Devices*, vol. 43, pp. 1732–1741, Oct. 1996.
[36] H. Mitlehner, W. Bartsch, M. Bruckmann, K. O. Dohnke, and U. Weinert, "The potential of fast high voltage SiC diodes," in *Proc. 9th Int. Symp. Power Semiconductor Devices and ICs*, 1997, pp. 165–168.
[37] V. Saxena and A. J. Steckl, "High voltage 4H SiC rectifiers using Pt and Ni metallization," *Mater. Sci. Forum*, vol. 264–268, pp. 937–940, 1998.
[38] R. Singh and J. W. Palmour, "Planar terminations in 4H–SiC Schottky diodes with low leakage and high yields," in *Proc. 9th Int. Symp. Power Semiconductor Devices and ICs*, 1997, pp. 157–160.
[39] Q. Wahab, T. Kimoto, A. Ellison, C. Hallin, M. Tuominen, R. Yakimova, A. Henry, J. P. Bergmann, and E. Janzen, "A 3 kV Schottky barrier diode in 4H–SiC," *Appl. Phys. Lett.*, vol. 72, no. 4, pp. 445–447, Jan. 1998.
[40] K. J. Schoen, J. M. Woodall, J. A. Cooper Jr., and M. R. Melloch, "Design considerations and experimental analysis of high-voltage SiC Schottky barrier rectifiers," *IEEE Trans. Electron Devices*, vol. 45, pp. 1595–1604, July 1998.
[41] V. Khemka, T. P. Chow, and R. J. Gutmann, "Effect of reactive ion etch-damage on the performance of 4H–SiC Schottky barrier diodes," *J. Electron. Mater.*, vol. 27, no. 10, pp. 1128–1135, Oct. 1998.
[42] H. Mitlehner, P. Friedrichs, D. Peters, R. Schorner, U. Weinert, B. Weis, and D. Stephani, "Switching behavior of fast high voltage SiC pn diodes," in *Proc. 10th Int. Symp. Power Semiconductor Devices and ICs*, 1998, pp. 127–130.
[43] J. H. Zhao, K. Tone, S. R. Weiner, M. A. Caleca, D. Honghua, and S. P. Withrow, "Evaluation of ohmic contacts to p-type 6H–SiC created by C and Al co implantation," *IEEE Electron Device Lett.*, vol. 18, pp. 375–377, Aug. 1997.
[44] M. E. Levinshtein, J. W. Palmour, S. L. Rumyantsev, and R. Singh, "turn-on process in 4H–SiC thyristors," *IEEE Trans. Electron Devices*, vol. 44, pp. 1177–1179, July 1997.
[45] N. V. Dyakonova, M. E. Levinshtein, J. W. Palmour, S. L. Rumyantsev, and R. Singh, "Temperature dependence of turn-on process in 4H–SiC thyristors," *Electron. Lett.*, vol. 33, no. 10, pp. 914–915, 1997.
[46] P. Neudeck, W. Huang, and M. Dudley, "Breakdown degradation associated with elementary screw dislocations in 4H–SiC p+/n junction rectifiers," *Solid-State Electron.*, vol. 42, no. 12, pp. 2157–2164, Dec. 1998.
[47] H. Yano, T. Kimoto, H. Matsunami, M. Blasser, and G. Pensl, "MOSFET performance of 4H-, 6H-, and 15R–SiC processed by dry and wet oxidation," *Mater. Sci. Forum*, vol. 338-342, pp. 1109–1112, Oct. 1999.
[48] G. Y. Chung, C. C. Tin, J. R. Williams, J. K. McDonald, M. Di Vantra, S. T. Pantelides, L. C. Feldman, and R. A. Weller, "Effect of nitride oxide annealing on the interface trap densities near the band edges in the 4H polytype of silicon carbide," *Appl. Phys. Lett.*, vol. 76, no. 13, pp. 1713–1715, Mar. 2000.
[49] L. Lipkin, "N2O processing improves the 4H–SiC : SiO2 interface," presented at the ICSCRM, Tsukuba, Japan, Oct.-Nov. 2001.
[50] D. Stephani, "Status, prospects and commercialization of SiC power devices," presented at the 59th Annu. Device Research Conf., South Bend, IN, June 2001.
[51] *Proc. Materials Research Society*, vol. 640, Silicon Carbide—Materials, Processing, and Devices, Boston, MA, 2000.
[52] A. Elasser, M. Ghezzo, N. Krishnamurty, J. Kretchmer, A. W. Clock, D. M. Brown, and T. P. Chow, "Switching characteristics of silicon carbide power p–i-n diodes," *Solid-State Electron.*, vol. 44, no. 2, pp. 317–323, Feb. 2000.
[53] H. Kapels, R. Rupp, L. Lorenz, and I. Zverev, "SiC Schottky diodes: A milestone in hard switching applications," in *Proc. Power Conversion and Intelligent Motion Conf.*, Nuremberg, Germany, June 2001, pp. 95–100.
[54] W. Wright, J. Carter, P. Alexandrov, P. Pan, M. Weiner, and J. H. Zhao, "Comparison of Si and SiC diodes during operation in three-phase inverter driving ac induction motor," *Electron. Lett.*, vol. 37, no. 12, pp. 787–788, June 2001.

[55] W. Wondrak, R. Held, E. Niemann, and U. Schmid, "SiC devices for advanced power and high-temperature applications," *IEEE Trans. Ind. Electron.*, vol. 48, no. 2, pp. 307–308, Apr. 2001.
[56] K. Shenai, P. Neudeck, and G. Schwarze, "Design and technology of compact high power converters," *IEEE Aerosp. Electron. Syst. Mag.*, vol. 16, pp. 27–31, Mar. 2001.
[57] C. M. Johnson <etal>, "Recent progress and current issues in SiC semiconductor devices for power applications," *IEE Proc. Circuits Devices Systems*, vol. 148, no. 2,, pp. 101–108, Apr. 2001.
[58] R. Rupp, "SiC Schottky diodes reach the market," *Compound Semiconductor Mag.*, vol. 7, no. 3, Apr. 2001.
[59] "Microsemi launches second-generation line of silicon carbide power Schottkies," *Compound Semiconductor Mag.*, press release, May 16, 2001.
[60] T. P. Chow, "SiC and GaN high-voltage power switching devices," in *Proc. Int. Conf. Silicon Carbide and Related Materials*, Research Triangle Park, NC, 1999, pp. 1155–1160.
[61] J. Wang and B. W. Williams, "Evaluation of high-voltage 4H–SiC switching devices," *IEEE Trans. Electron Devices*, vol. 46, pp. 589–597, Mar. 1999.
[62] M. J. Schutten and D. A. Torrey, "Edge-resonant power converter with novel magnetics," in *Proc. IEEE Power Electronics Specialist Conf.*, June 1997, pp. 769–774.
[63] M. J. Schutten, M. Kheraluwala, R. L. Steigerwald, and D. A. Torrey, "EMI comparison of hard switched, edge-resonant and load resonant dc/dc converters using a common power stage," in *Proc. IEEE Industry Applications Society Conf.*, vol. 2, 1998, pp. 1588–1595.
[64] V. Vlatkovic, M. J. Schutten, and R. Steigerwald, "Auxiliary series resonant converter: A new converter for high-voltage, high-power applications," in *Proc. IEEE Applied Power Electronic Conf.*, 1996, pp. 493–499.
[65] High Voltage Diode Data Sheet, Philips. [Online]. Available: http://www.semiconductors.philips.com/acrobat/datasheets/ BY8100_2.pdf
[66] Y. Sugawara, D. Takayama, K. Asano, R. Singh, J. Palmour, and T. Hayashi, "12—19kV 4H–SiC pin diodes with low power loss," in *Proc. Int. Symp. Power Semiconductor Devices and ICs*, 2001, pp. 27–30.
[67] K. Shenai and M. Trivedi, "Silicon carbide power electronics for high temperature applications," in *Proc. IEEE Aerospace Conf.*, vol. 5, 2000, pp. 431–437.
[68] P. G. Neudeck, "Progress toward high temperature, high power SiC devices," in *Proc. Inst. Phys. Conf.*, vol. 141, Compound Semiconductors, 1994, pp. 1–6.
[69] R. Sei-Hyung, A. K. Agarwal, J. W. Palmour, and M. E. Levinshtein, "1.8 kV, 3.8 A bipolar junction transistors in 4H–SiC," in *Proc. 13th Int. Symp. Power Semiconductor Devices and ICs*, 2001, pp. 37–40.
[70] M. R. Werner and W. R. Fahrner, "Review on materials, microsensors, systems, and devices for high-temperature and harsh-environment applications," *IEEE Trans. Ind. Electron.*, vol. 48, pp. 249–257, Apr. 2001.
[71] Benefits of silicon carbide electronics to aircraft, NASA. [Online]. Available: http://www.grc.nasa.gov/WWW/SiC/aircraftbenefit.html
[72] N. G. Hingorani, "High-voltage dc transmission: A power electronics workhorse," *IEEE Spectrum*, vol. 33, pp. 63–72, Apr. 1996.
[73] E. R. Brown, "Megawatt solid-state electronics," *Solid-State Electron.*, vol. 42, no. 12, pp. 2119–2130, 1998.
[74] M. M. Freeman and M. R. Perschbacher, "Hybrid power—an enabling technology for future combat systems," in *Proc. 12th IEEE Int. Pulsed Power Conf.*, vol. 1, 1999, pp. 17–22.
[75] M. Ghezzo, "Silicon carbide megawatt power devices for combat vehicles," General Electric CRD, Final Rep. DARPA Contract MDA972-98-C-0001, July 2001.
[76] T. Burke, K. Xie, J. R. Flemish, H. Singh, T. Podelsak, and J. H. Zhao, "Silicon carbide power devices for high temperature, high power density switching applications," in *Proc. IEEE 22nd Power Modulator Symp.*, 1996, pp. 18–21.
[77] T. Burke, K. Xic, H. Singh, T. Podlesak, and J. Flemish, "Silicon carbide thyristors for electric guns," *IEEE Trans. Magn.*, vol. 33, pp. 432–437, Jan. 1997.
[78] A. Welleman, U. Schlapbach, and E. Ramezani, "Plug and play solid state switching system for laser applications," in *Proc. 12th IEEE Int. Pulsed Power Conf.*, vol. 1, 1999, pp. 150–152.
[79] Y. Chung, C. Yang, and H. Kim, "All solid state switched pulser for air pollution control system," in *Proc. 12th IEEE Int. Pulsed Power Conf.*, vol. 1, 1999, pp. 177–180.
[80] T. F. Podlesak and F. M. Simon, "Single shot and burst repetitive operation of involute gate 125mm symmetric thyristors up to 221kA with a di/dt of 2k A/ s," in *Proc. 12th IEEE Int. Pulsed Power Conf.*, vol. 1, 1999, pp. 206–209.
[81] C. R. Hummer, H. Singh, and D. Piccone, "Thyristors for pulsed power applications," in *Proc. 24th Int. Power Modulator Symp.*, 2000, pp. 78–80.
[82] R. B. True, R. J. Hansen, and G. R. Good, "The Hobetron-a high power vacuum electronic switch," *IEEE Trans. Electron Devices*, vol. 48, pp. 122–128, Jan. 2001.

Ahmed Elasser (Member, IEEE) was born in Demnate, Morocco, in 1963. He received the B.S. degree in electric power engineering from Mohammadia School of Engineering, Rabat, Morocco, in 1985 and the M.S. and Ph.D. degrees in electric power engineering and power electronics from Rensselaer Polytechnic Institute, Troy, NY, in 1996.

He was an Electrical Maintenance Engineer and then a Laboratory Engineer from 1986 to 1992. In 1996, he joined the General Electric (GE) Global Research Center, Niskayuna, NY, as a Senior Professional. He has authored or coauthored more than fifteen papers, holds four patents, and has a number of other patents pending. His previous research interests include the study, modeling, and application of power semiconductor devices, systems modeling and simulation, silicon carbide devices, six-sigma quality, and e-engineering. His current research interests include silicon carbide power devices' modeling, testing, characterization, and potential applications.

Dr. Elasser received the Dushman Team Award from GE in 1996 in addition to other awards from GE Industrial Systems. He is a regular reviewer for the IEEE TRANSACTIONS ON POWER ELECTRONICS.

T. Paul Chow (Senior Member, IEEE) received the B.A. degree in mathematics and physics (*summa cum laude*) from Augustana College, Sioux Falls, SD, in 1975, the M.S. degree in materials science from Columbia University, New York, NY, in 1977, and the Ph.D. degree in electrical engineering from Rensselaer Polytechnic Institute, Troy, NY, in 1982.

From 1977 to 1989, he was with General Electric Corporate Research and Development, Schenectady, NY, where he was involved with doped tin–oxide thin films for transparent electrode applications in solid-state imagers and with refractory metals and metal silicides for metal-oxide semiconductor (MOS) very large scale integration applications. From 1982 to 1989, he participated in the development of various discrete and integrable MOS-gated unipolar and bipolar power devices and high-voltage integrated circuits. In 1989, he joined the Department of Electrical, Computer, and Systems Engineering, Rensselaer Polytechnic Institute, where he is currently a Professor. Since 1998, he has led the Advanced Semiconductor Power Devices subthrust for the Center for Power Electronics Systems—an Engineering Research Center consortium led by Virginia Tech and sponsored by the National Science Foundation. He has authored or coauthored over 80 papers in journals, presented over 100 conference talks, contributed four chapters in technical textbooks, and holds over ten patents. His current research interests include developing new device concepts for high-voltage power devices and integrated circuits and in process research of wide bandgap compound semiconductors.

Dr. Chow is a Member of the Electrochemical Society and an AdCom Member of the IEEE Electron Devices Society. He received the Solid-State Science and Technology Young Author Award of the Electrochemical Society in 1982 and the Horizon Award from Augustana College in 1986. He was an Associate Editor of IEEE TRANSACTIONS ON ELECTRON DEVICES.